

Improvement of the KarstMod modeling platform for a better assessment of karst groundwater resources

Vianney Sivellev¹, Guillaume Cinkus^{1,2}, Naomi Mazzilli², David Labat³, Bruno Arfib⁴, Nicolas Massei⁵,
Yohann Cousquer¹, Dominique Bertin⁶, and Hervé Jourde¹

¹HSM, Univ Montpellier, CNRS, IRD, Montpellier, France

²EMMAH, INRAE, Avignon Université, 84000 Avignon, France

³Geosciences Environment Toulouse UMR CNRS IRD Université Paul Sabatier CNES, 14 Avenue Edouard Belin 31400 TOULOUSE

⁴Aix-Marseille Univ, CNRS, IRD, INRAE, Coll de France, CEREGE, Aix-en-Provence, France

⁵Univ Rouen Normandie, Univ Caen Normandie, CNRS, M2C, UMR 6143, F-76000 Rouen, France ⁶GEONOSIS, France

Correspondence: vianney.sivelle@umontpellier.fr

Abstract.

Hydrological models are fundamental tools for the ~~characterisation~~ **characterization** and management of karst systems. We propose an updated version of KarstMod, a software dedicated to lumped parameter rainfall-discharge modeling of karst aquifers. KarstMod provides a modular, user-friendly modeling environment for educational, research, and operational purposes. It also includes

5 numerical tools for time series analysis, model evaluation, and sensitivity analysis. The modularity of the platform facilitates common operations related to lumped parameter rainfall-discharge modeling, such as (i) ~~set-up~~ **setup** and parameter estimation of a relevant model structure, and (ii) evaluation of internal consistency, parameter sensitivity, and hydrograph characteristics. The updated version now includes (i) external routines to better consider the input data and their related uncertainties, i.e. evapotranspiration and solid precipitation, (ii) enlargement of multi-objective calibration possibilities, allowing more flexibility in

10 terms of objective functions as well as observation type and (iii) additional tools for model performance evaluation including further performance criteria and tools for model errors representation.

1 Introduction

~~Karst systems consist of heterogeneous aquifers characterized with the co-existence of three types of porosity: (i) intergranular porosity, (ii) fracture porosity and (iii) large voids and conduits (Palmer, 1991; White, 1999) characterized by contrasted hydrodynamic properties. The existence of surface karst features such as shafts or swallow holes often leads to concentrated point source recharge towards karst conduits in addition to the more common homogeneous diffuse recharge over the~~

Définition du style : Normal: Interligne : Multiple 1,43

a mis en forme : Espace Après : 1,2 pt

a mis en forme : Italien (Italie)

a mis en forme : Italien (Italie), Exposant

a mis en forme : Italien (Italie)

a mis en forme : Français (France)

a mis en forme : Retrait : Gauche : 0,84 cm, Espace Après : 2,35 pt, Interligne : Multiple 1,08 li

a mis en forme : Espace Après : 12,4 pt

a mis en forme : Espace Après : 20,7 pt

~~catchment. It also implies that flow regimes can be either laminar or turbulent.~~ Karst aquifers constitute an essential source of drinking water for about 9.2% of the world population (Stevanovic, 2019) and it is estimated that one-quarter of the world population depends on freshwater from karst aquifers (Ford and Williams,

15 2013). Karst aquifers contain an important ~~volume~~ of freshwater while only 1% of its annually renewable water is used for drinking water supply (Stevanovic, 2019). ~~Karst groundwater thus represents an unique opportunity to limit the imbalance between growing demand and limited freshwater resource (Wada et al., 2016; Bierkens and Wada, 2019), particularly in areas where no other freshwater resources are identified. However, karst aquifers are also particularly vulnerable to potential sources of contamination, including emergent contaminants (Lukac Reberski et al., 2022), residues of phyto-sanitary products (Lorette et al., 2022) and wastewater (Doummar et al.,~~

25 2022). Understanding the functioning of karst aquifers and developing operational tools to predict the evolution of freshwater resources is therefore a major challenge for the hydrological science community (Blöschl et al., 2019). ~~Such~~ To this day, the number of tools dedicated to karst hydrogeology is limited and is mostly developed for academic purposes and not user-friendly. Nonetheless, such tools are also required for a better assessment of groundwater vulnerability as ~~well as sustainable management of the groundwater resources (Elshall et al., 2020).~~

well as sustainable management of the groundwater resources (Elshall et al., 2020) and should be handled by the stakeholders without programming skills requirements.

KarstMod is an adjustable modeling platform (Mazzilli et al., 2019) dedicated to lumped parameter rainfall-discharge ~~mod~~ modeling allowing for (i) simulation of spring discharge, piezometric head and surface water discharge (Sophocleous, 2002; Bailly-

30 ~~eling allowing for (i) simulation of spring discharge, piezometric head~~ Comte et al., 2012; Cousquer and surface discharge, Jourde, 2022), (ii) hydrodynamic analysis of the internal fluxes considered in the model, (iii) model performance perfor-

35 ~~mance~~ evaluation and parametric sensitivity analysis. In this paper, we present the new features incorporated in KarstMod: (i) external routines to better consider the input data and their related uncertainties, i.e. evapotranspiration and solid precipitation, (ii) enlargement of multi-objective calibration possibilities, allowing more flexibility in terms of objective functions as well as observation type with the possibility to include surface water

40 discharge in the calibration procedure and (iii) model performance evaluation, including additional performance criteria as well as additional tools for model errors representation such as

30 the diagnostic efficiency plot (Schwemmler et al., 2021). Also, we present two case studies to illustrate how KarstMod is useful in the framework of the assessment of karst groundwater resources and its sensitivity to groundwater abstraction. Section 2 is devoted to the presentation of the background and motivations to improve the functionalities of the platform while Sect. 3 presents the main features of KarstMod. Section 4 illustrates the

a mis en forme : Police :8,5 pt

a mis en forme : Gauche, Retrait : Gauche : 0,85 cm, Première ligne : 0,35 cm, Droite : 0 cm, Espace Après : 0 pt, Interligne : simple

a mis en forme : Police :10 pt

a mis en forme : Police :8,5 pt

a mis en forme : Retrait : Gauche : 0,19 cm, Première ligne : 0 cm, Espace Après : 20,7 pt

presents the main features of KarstMod. ~~49~~Section 4 illustrates the application of rainfall-discharge modeling using KarstMod within the Touvre (western France) and the Lez (southern France) karst systems, which both constitute strategic ~~fresh~~ ~~water-freshwater~~ ~~35~~ resources and ensure drinking water supply.

a mis en forme : Police :10 pt

a mis en forme : Police :8,5 pt

2 Background and motivations

2.1 Challenges in karst groundwater resources

Karst aquifers are affected by the combination of different components of global change such as (i) effects of climate change ~~45~~ which are particularly pronounced in the Mediterranean area (Dubois et al., 2020; Nerantzaki and Nikolaidis, 2020), (ii) ~~increasing in-~~

a mis en forme : Police :10 pt

~~40~~ ~~creasing~~ groundwater abstraction (Labat et al., 2022), as well as (iii) changes in land cover land use (Bittner et al., 2018; Sarrazin et al., 2018). Therefore, the assessment of karst groundwater resources ~~vulnerability in the present context~~ ~~sensitivity in terms of quantity~~, requires operational tools for estimating the sustainable yield of karst aquifers but also to predict the impacts of climatic or anthropogenic forcing on groundwater resources in the long term (Sivelle et al., 2021). ~~In order to~~ ~~To~~ address these issues, different

~~50~~ modeling approaches have been developed (Jeannin et al., 2021) such as, among others, fully-distributed models (Chen and Goldscheider, 2014),

a mis en forme : Police :10 pt

~~45~~ semi-distributed models (Doummar et al., 2012; Dubois et al., 2020; Ollivier et al., 2020), and lumped parameter models (Mazzilli et al., 2019) including semi-distributed recharge (Bittner et al., 2018; Sivelle et al., 2022a). Among these, lumped parameter models are recognized as major tools to explore the ability of conceptual representations to explain observations in karst systems (Poulain et al., 2018; Sivelle et al., 2019; Duran et al., 2020; Frank et al., 2021) and for managing ~~55~~ karst groundwater resources (Sivelle and Jourde, 2020; Sivelle et al., 2021; Labat et al., 2022; Cousquer and Jourde, 2022).

a mis en forme : Police :8,5 pt

a mis en forme : Espace Après : 0 pt

~~50~~ 2.2 Challenges in lumped parameters modeling in karst hydrology

a mis en forme : Taquets de tabulation : Pas à 1,07 cm

Lumped parameter models consist of a functional approach that analyzes ~~an~~ hydrogeological system at the catchment scale and describes the transformation from rainfall into discharge using empirical or conceptual relationships. Therefore, parameter values or distributions cannot be determined directly from catchment physical characteristics or *in-situ* measurements, ~~excepted~~ ~~except the discharge coefficient to the spring that can be estimated based on recession curve analysis. Instead, model parameter~~ ~~60~~ ~~the discharge coefficient to the spring that can be estimated on the basis of recession curve analysis. Instead, model~~ ~~parameters~~ ~~55~~ values must be estimated by history-matching. In a general way, rainfall-discharge models in karst hydrology are calibrated considering spring discharge measurements.

a mis en forme : Police :8,5 pt

Former studies have shown the interest of considering various types of observations such as natural hydro-chemical tracers:

~~NO₃~~ and SO₄ concentrations (Hartmann et al., 2013), electrical conductivity (Chang et al., 2021) or excess air (Sivelle et al., 2022b).

~~65-2022b~~ Indeed, the consideration of complementary observation data in groundwater model calibration appears relevant in many applications

60 cations (Schilling et al., 2019) but requires additional investigations before a suitable implementation in KarstMod. Therefore, in this paper, we will focus on the use of hydrodynamics observations only. Indeed, considering piezometric head variations in lumped parameters rainfall-discharge models may lead to better model performance (Mazzilli et al., 2011; Cousquer and Jourde, 2022). Nonetheless, the information content of the piezometric head time series (directly measured, or

~~70~~ derived from ground-based gravity measurements) for lumped parameters rainfall-discharge models calibration purpose can be disputable

~~65~~ when the available data is not adequate to characterize the whole catchment due to the important heterogeneity in karst aquifers (Sivelle and Jourde, 2020; Mazzilli et al., 2013). Also, Cousquer and Jourde (2022) ~~account~~ accounts for the surface runoff-water discharge in a lumped parameters rainfall-discharge model calibration procedure allowing for to ~~reducereduction of~~ the parametric uncertainties.

Another key point in lumped parameter rainfall-discharge modeling concerns the evaluation of the meteorological forcing, ~~75~~ i.e. precipitation (*P*) and evapotranspiration (*ET*). The transformation of precipitation into recharge and finally into discharge

~~70~~ includes several processes with characteristic times covering several orders of magnitude (Blöschl and Sivapalan, 1995). Thus, the temporal resolution of the hydrological model must be suitable in the range of time and space scale where the physical ~~phenomenonsphenomena~~ take place. Coupling hydrological models at multiple temporal resolutions can provide a better model consistency (Sivelle et al., 2019) since the transfer function in karst aquifers may present a short response time. Also, errors in rainfall

~~80~~ time series can significantly affect model parameters and structure (Oudin et al., 2006). Finally, the response of karst spring

~~75~~ discharge is sensitive to energy and water fluxes within the soil-vegetation-atmosphere (SVA) continuum as well as changes in climatic conditions (Hartmann et al., 2017). Bittner et al. (2021) computed several models to evaluate the fluxes related to interception, evapotranspiration, and snow process. The results show significant uncertainties related to input data as well as potential compensation between the various uncertain processes. In some cases, snow melt is a controlling factor in the water balance (Doummar et al., 2018a; Liu et al., 2021), thus a suitable snowmelt estimation is required to improve hydrological

~~8580~~ balance (Doummar et al., 2018a; Liu et al., 2021), thus a suitable snow-melt estimation is required to improve hydrological model performance (Çalli et al., 2022). Therefore, two meteorological modules have been added to KarstMod: (i) a "Snow

a mis en forme : Gauche, Retrait : Gauche : 0,85 cm, Première ligne : 0,35 cm, Droite : 0 cm, Espace Après : 0 pt, Interligne : simple

a mis en forme : Police :10 pt

a mis en forme : Police :8,5 pt

a mis en forme : Police :10 pt

a mis en forme : Police :8,5 pt

a mis en forme : Police :10 pt

a mis en forme : Police :8,5 pt

a mis en forme : Police :10 pt

a mis en forme : Police :10 pt

a mis en forme : Police :8,5 pt

a mis en forme : Espace Après : 0 pt

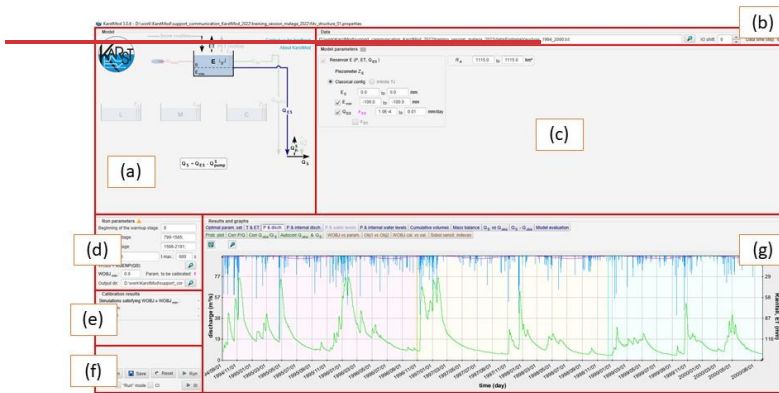
routine" and (ii) a routine to compute the potential evapotranspiration (*PET*), denoted "PET routine". The two additional modules allow us to better account for snow and evapotranspiration processes.

3 Implementation

90 The updated version of KarstMod implements additional features to enhance the rainfall-discharge modeling practices. First,

85 we describe the additional modules (snow and PET routines) for a better meteorological forcing estimation. Then, we introduce the additional tools proposed for (i) the set-up/setup and calibration of the model structure, (ii) model performance evaluation as well as (iii) uncertainties consideration. Figure 1 shows a screenshot of the KarstMod software.

a mis en forme : Police :8,5 pt



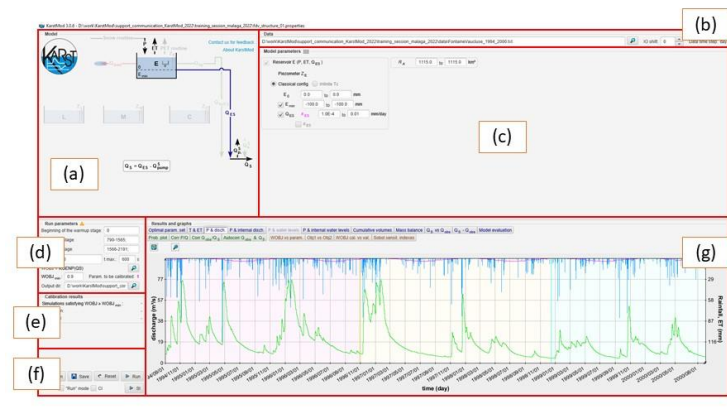


Figure 1. Screenshot of the KarstMod software with: (a) model structure, (b) data import, (c) model parameters, (d) run parameters, (e) calibration results, (f) command bar, and (g) results and graphs.

3.1 Meteorological modules

3.1.1 Snow routine

KarstMod allows using either observation-based precipitation time series P [$L T^{-1}$] or estimated precipitation time series P_{sr} [$L T^{-1}$] using a snow routine. The latter is similar to the one used by Chen et al. (2018) – without the radiation components – which has been successfully used for improving the simulation of karst spring discharge in snow-covered karst systems (Chen et al., 2018; Cinkus et al., 2023b). It consists of a modified HBV-snow routine (Bergström, 1992) for simulating snow accumulation and melt over different sub-catchments based on altitude ranges (appendix A). Each sub-catchment is defined by two values that the user must input: (i) the proportion among the whole catchment (sum must be equal to 1) and melt over (ii) the temperature shift, related to the altitude gradient. The different sub-catchments based on altitude ranges (appendix A). The estimated precipitation P_{sr} associated with the subcatchments are calculated and summed to produce the estimated precipitation time series P_{sr} , which corresponds to a single variable representative of the catchment. P_{sr} thus gives the water leaving the snow routine, and is equivalent to the recharge into the first compartment of the model (compartment E in KarstMod). P_{sr} for each sub-catchment is proportional to its surface regarding the complete catchment area. The snow routine workflow requires both air temperature

a mis en forme : Espace Après : 15,8 pt

a mis en forme : Espace Après : 15,1 pt

a mis en forme : Taquets de tabulation : 1,2 cm,

a mis en forme : Retrait : Gauche : 0,17 cm, Suspensu : 0,69 cm, Espace Après : 0 pt, Interligne : simple

a mis en forme : Police :Calibri, Non Italique

100 T [$^{\circ}\text{C}$] and precipitation P [L T^{-1}] time series. P is considered as snow when T in the sub-catchment is lower than the temperature threshold T_s . Snow melt starts when the temperature exceeds the threshold
 105 according to a degree-day expression. The snow melt is a function of the melt coefficient MF [$\text{L T}^{-1} \cdot \text{C}^{-1}$], and the degrees above the temperature threshold $-T_s$. Runoff starts when the liquid water holding capacity of snow CWH [-] is exceeded. The refreezing coefficient CFR [-] stands for refreezing liquid water in the snow when snow melt is interrupted (Bergström, 1992). The output of the snow routine consists of a redistributed precipitation time series P_{sr} . The four parameters of the snow routine

105 of a redistributed precipitation time series P_{sr} . The four parameters of the snow routine (i.e. T_s , MF , CWH and CFR) can be considered in the parameter estimation procedure as well as sensitivity analysis. The snow routine features can be activated from the model structure area (Figure 1a).

3.1.2 PET routine

An additional module allows to compute PET based on the Oudin's formula (Oudin et al., 2005). The PET routine can be activated from the model structure area (Figure 1a). Then, KarstMod allows to consider water transfer between in the soil-atmosphere continuum in four different ways (Figure 2):
 115-120 activated from the model structure area (Figure 1a). Then, KarstMod allows us to consider water transfer in the soil-atmosphere continuum in four different ways (Figure 2):

(a) Effective precipitation time series (P_{eff}) can be pre-processed by the user (Eq. 1) and the evapotranspiration flux is not activated in the model structure selection window in KarstMod (1a).

$$P_{eff} = P - ETa$$

115 where P_{eff} is effective precipitation [L T^{-1}], P is precipitation [L T^{-1}] and ETa is user-defined actual evapotranspiration [L T^{-1}] computed by observation-based data or external model. evapotranspiration [L T^{-1}] computed by observation-based data or external model.
 120 (b) User-defined PET can be given as input in KarstMod for the evapotranspiration time series. Compartment E stands for soil and epikarst storage zone, where water is available for actual evapotranspiration (ETa), and flows to the lower level of the model structure or outflow as surface discharge losses. Using E_{min} , the user can simulate water holding capacity and non-linear behavior of karst recharge.

a soil and epikarst storage zone, where water is available for actual evapotranspiration (ETa), flows to lower level of the model structure or outflow as surface discharge losses. Using E_{min} , user can simulate water holding capacity and non-linear behavior of karst recharge.

a mis en forme : Police :8,5 pt

a mis en forme : Police :10 pt

a mis en forme : Espace Après : 0 pt

a mis en forme : Police :Calibri, Non Italique

a mis en forme : Retrait : Gauche : -0,03 cm, Suspendu : 0,87 cm, Droite : -0,03 cm, Espace Après : 10,4 pt, Interligne : Multiple 1,39 li

a mis en forme : Police :10 pt

a mis en forme : Droite, Retrait : Gauche : 0,02 cm, Droite : -0,03 cm, Espace Après : 3,85 pt, Interligne : Multiple 1,08 li

a mis en forme : Retrait : Gauche : 0,85 cm, Suspendu : 0,88 cm, Espace Après : 7,15 pt, Interligne : simple

a mis en forme : Espace Après : 11,8 pt

a mis en forme : Retrait : Gauche : -0,03 cm, Espace Après : 5,15 pt, Interligne : Multiple 1,08 li, Taquets de tabulation : 18,55 cm, Droite

a mis en forme : Retrait : Suspendu : 0,57 cm, Espace Après : 7,3 pt, Interligne : simple, Numéros + Niveau : 1 + Style de numérotation : a, b, c, ... + Commencer à : 2 + Alignement : Gauche + Alignement : 0,98 cm + Retrait : 0,98 cm

(e) User-defined actual evapotranspiration (ETa) can be given as input data in KarstMod for evapotranspiration time series instead of potential evapotranspiration. KarstMod computes effective precipitation by limiting the evapotranspiration to water content available in compartment E; calculated actual evapotranspiration can then be lower than the user's input ETa .

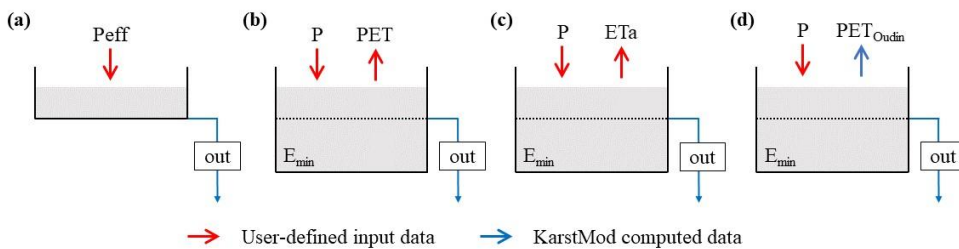
(d) The new feature in KarstMod is the PET routine which estimates the potential evapotranspiration based on the Oudin's formula (Oudin et al., 2005) (Eq. 2). It needs a temperature time series and two parameters to be estimated, which can be considered in the parameter estimation procedure as well as sensitivity analysis.

$$PET = \frac{R_e}{\lambda \cdot \rho} \times \frac{T + K2}{K1} \quad \text{if } T + K2 > 0 \quad \text{else } PET = 0$$

$$PET = \frac{R_e}{\lambda \cdot \rho} \times \frac{T + K2}{K1} \quad \text{if } T + K2 > 0 \quad \text{else } PET = 0$$

(2)

where R_e is the extraterrestrial radiation [$\text{MJ L}^{-2} \text{T}^{-1}$] depending only on latitude Lat and Julian day, λ is the latent heat flux (taken equal to 2.45 MJ M^{-1}), ρ is the density of water [M L^{-3}] and T is the mean daily air temperature [$^{\circ}\text{C}$]. The latter is a single function of the Julian day for a given location. $K1$ [$^{\circ}\text{C}$] and $K2$ [$^{\circ}\text{C}$] are constants to adjust over the catchment for rainfall-discharge model (Oudin et al., 2005). In KarstMod, both $K1$ and $K2$ can be considered in the parameter estimation procedure as well as sensitivity analysis.



a mis en forme : Retrait : Suspendu : 0,57 cm, Espace Après : 7,65 pt, Interligne : simple, Numéros + Niveau : 1 + Style de numérotation : a, b, c, ... + Commencer à : 2 + Alignement : Gauche + Alignement : 0,98 cm + Retrait : 0,98 cm

a mis en forme : Retrait : Gauche : 1,75 cm, Première ligne : 0 cm

a mis en forme : Droite : -0,03 cm, Espace Après : 6 pt

a mis en forme : Retrait : Gauche : -0,03 cm, Première ligne : 1,73 cm, Espace Après : 6,95 pt

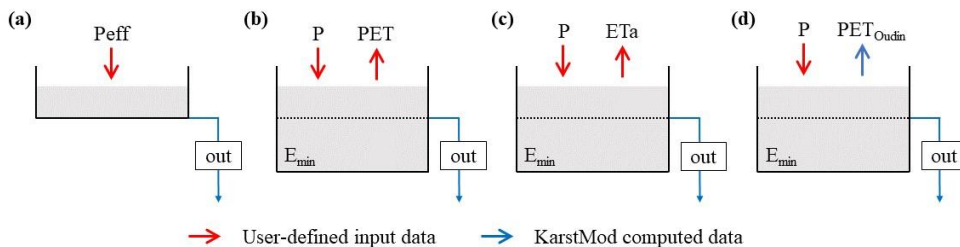


Figure 2. The four ways to account for evapotranspiration in KarstMod. The user can ~~prevides~~provide either (a) a self-computed effective precipitation ($P - ETa$) as a single input time series, (b) both P and PET time series, (c) both P and ETa and (d) both P and T time series. P is precipitation, ETa is actual evapotranspiration, PET is potential evapotranspiration and PET_{Oudin} is KarstMod's computed potential evapotranspiration with Oudin's formula.

3.2 Set up and calibration of the model structure

~~135~~ The modular structure proposed in KarstMod is based on a widely used conceptual model which separates karst aquifers into an infiltration zone and a saturated zone, or low and quick flows through the unsaturated and saturated zones (Fleury et al.,

~~2007, 2009; Guinot et al., 2015; Mazzilli et al., 2019; Sivelles et al., 2019~~). Based on this conceptual representation, the platform

~~140~~ offers four compartments organized as a two-level structure: (i) compartment E (higher level) and (ii) compartments L, M and C

(lower level). A priori, the higher-level ~~stands for~~represents the infiltration zone or the soil and epikarst. At the lower level, compartments

~~140~~ L, M, and C stand for the different sub-systems of the saturated zone, or ~~for~~low and quick flows of the whole ~~hydro~~systemhydro system. The various model structures and their governing equations are presented in Mazzilli et al. (2019, 2022). Also, KarstMod allows to ~~perform~~performance of hydrological modeling on both daily and hourly temporal resolutions (Sivelles et al., 2019).

~~145~~ The user can activate (or deactivate) the various compartments (E, L, M, and C) within the "model structure" panel (Figure 1a). The solid and faded colors represent the activated and the inactivated features respectively. The fluxes and their activation

~~145~~ thresholds as well as the exponent of the discharge law α (in case of non-linear discharge law such $\alpha \neq 1$) are managed from the "model parameters" panel (Figure 1c). The user can account for pumping Q_{pump} (water coming out of the compartment)

a mis en forme : Gauche, Retrait : Gauche : 0,84 cm, Espace Après : 0 pt

a mis en forme : Police :10 pt

a mis en forme : Retrait : Gauche : -0,03 cm, Suspendu : 0,85 cm, Espace Après : 0 pt, Interligne : simple

a mis en forme : Police :8,5 pt

a mis en forme : Retrait : Gauche : -0,03 cm, Suspendu : 0,85 cm

a mis en forme : Police :8,5 pt

a mis en forme : Retrait : Gauche : -0,03 cm, Suspendu : 0,87 cm, Droite : -0,03 cm, Espace Après : 1,3 pt, Interligne : Multiple 1,39 li

as well as sinking stream Q_{sink} (water coming into the compartment). Such an option is available only if the user provides the ~~150~~ required time series (Figure 1b).

The user must provide the warm-up, calibration, and validation periods (Figure 1d). The warm-up period must be set ~~in~~ order to be 150 independent ~~from~~ initial conditions to avoid bias in the parameter estimation procedure (Mazzilli et al., 2012). Then, a calibration period (i.e. the period in which the ~~parameter~~ parameters are estimated to reduce the predictive errors) and a validation period

(i.e. period separated from the calibration period) can be defined to run the split sample test procedure (Klemeš, 1986). For

~~155~~ calibration purpose, KarstMod proposes several widely used performance criteria ϕ : the Pearson's correlation coefficient r_p

(Freedman et al., 2007), the Spearman rank correlation coefficient r_s (Freedman et al., 2007), the Nash-Sutcliffe Efficiency NSE (Nash

~~155~~ and Sutcliffe, 1970), the volumetric error VE (Criss and Winston, 2008), the modified balance error BE (Perrin et al., 2001), the Kling-Gupta Efficiency KGE (Gupta et al., 2009) and a non-parametric variant of the Kling-Gupta Efficiency

~~160~~ $KGENP$ (Pool et al., 2018). To compute a multi-objective calibration procedure the user can create his own-objective function ~~160~~

Φ as a weighted sum of several objective functions:

$$\Phi = \sum_{i=1}^N \omega_i \times \phi_i(U) \quad (3)$$

~~160~~ where ω is the weight affected ~~to~~by the objective function $\phi(U)$ with $\sum \omega_i = 1$ and U a general notation for the observations used

for parameter estimation ~~purpose~~ purposes. In the KarstMod modeling platform, U corresponds to either spring discharge Q_s , piezometric head measurements Z (available for compartments E, L, M, and C), or surface water discharge Q_{loss} from com- ~~partments~~ partments E. Also, the objective function ϕ can be computed on transformed U to avoid high water level bias ~~on quadratic error.~~

~~error-~~ The following ~~transformation~~ transformations are available in KarstMod: $1/U$, \sqrt{U} , $1/\sqrt{U}$. Therefore, the user can use any combination of

~~165~~ the objective function ϕ , observations U , and variable transformations. Depending on the modeling purpose, the user must

refer to the literature to define the suitable objective function (Bennett et al., 2013; Ferreira et al., 2020; Hauduc et al., 2015; Jackson et al., 2019).

a mis en forme : Police :10 pt

a mis en forme : Police :10 pt

a mis en forme : Police :8,5 pt

a mis en forme : Police :10 pt

a mis en forme : Retrait : Gauche : -0,03 cm, Suspendu : 0,85 cm, Espace Après : 12,6 pt

a mis en forme : Espace Après : 8,35 pt

a mis en forme : Retrait : Gauche : -0,03 cm, Suspendu : 0,85 cm, Espace Après : 1,6 pt

a mis en forme : Retrait : Gauche : 0 cm

a mis en forme : Police :8,5 pt

a mis en forme : Police :Calibri, Non Italique

a mis en forme : Retrait : Gauche : -0,03 cm, Suspendu : 0,85 cm

170 The model is calibrated using a quasi-Monte-Carlo sampling procedure with a Sobol sequence sampling of the parameter space (Sobol, 1976). The procedure ~~consists in~~involves finding an ensemble of parameter ~~sets~~sets providing an objective function Φ greater

175 than the user-defined value. The calibration procedure is stopped when either the user-defined maximum duration t_{max} is* reached or the user-defined number of parameter set n_{max} are collected. KarstMod offers a "run" option allowing to run the model for a user-defined parameter set, without calibration procedure, and so ~~allowing~~allows to investigate "by-hand" the parameter-175 space and the sensitivity of the model to specific parameters.

3.3 Model evaluation

175 The model performance can be evaluated for both the calibration and validation periods. It allows (i) to ensure the robustness of model predictions, even under changing conditions (which is a key point for the assessment of climate change impact) and

(ii) to avoid model over-fitting within a specific range of hydro-climatic conditions observed during the calibration period. KarstMod allows the computation of the above-mentioned performance criteria for both calibration and validation periods.

~~180 KarstMod allows the computation of the above-mentioned performance criteria for both calibration and validation periods.~~ Even though the notation "validation" is disputable such a procedure is required to evaluate both explanatory and predictive

180 dimensions of the model structure (Andréassian, 2023). Then, KarstMod offers an ensemble of numerical tools devoted to (i) ~~check~~checking the model consistency, i.e. explanatory dimension of the model (Beven, 2001; Shmueli, 2010), (ii) ~~evaluate~~evaluating the model performance, i.e. predictive dimension of the model structure.

185 To check the model consistency, the simulation based on the parameter set that provides the highest objective function value can be analyzed through an ensemble of graphs such as (i) internal and external fluxes as a function of time, (ii) cumulative

185 volumes for both observed and simulated time series for spring discharge Q_s and surface water discharge Q_{loss} , (iii) simulated mass-balance as a function of time, (iv) comparison of observations and simulations for either Q_s or Q_{loss} with probability function plots, auto-correlogram of the spring discharge time series, cross-correlogram of precipitation-discharge time series.

190 To evaluate the model performance, KarstMod offers a "Model evaluation" panel available from the graphs panel* (Figure 1g) that includes several sub-panels, from the left to the right:

190 — The diagnostic efficiency DE (Schwemmlé et al., 2021) which consists of a diagnostic polar plot that facilitates the model evaluation process as well as the comparison of multiple simulations. The DE accounts for constant, dynamics, and timing errors, and their relative contribution to the model errors. Also, the decomposition of the errors between the 195 periods of high flows and low flows allows us to better investigate the model bias, as well as to provide critical evaluation

a mis en forme : Police :8,5 pt

a mis en forme : Retrait : Gauche : -0,03 cm, Suspendu : 0,85 cm

a mis en forme : Police :10 pt

a mis en forme : Retrait : Gauche : -0,03 cm, Suspendu : 0,85 cm, Espace Après : 0 pt, Interligne : simple

a mis en forme : Police :8,5 pt

a mis en forme : Police :8,5 pt

a mis en forme : Retrait : Gauche : 0,85 cm, Première ligne : 0,35 cm, Espace Après : 8,85 pt

195 for impact studies, particularly for the assessment of climate change impacts. Indeed, the accurate evaluation of low flow periods (in terms of frequency, intensity, and duration) becomes more and more crucial for groundwater resource variability assessment.

200 – The available objective functions ϕ are presented as a radar chart which consists of a polygon where the position of each point from the center gives the value of the performance criteria. The closer the point is to the outside of the radar chart, the better the model performs. The radar chart is made for both calibration and validation periods and for each of the 200 calibration variables considered in the modeling (Q_{obs}^A, Z_{obs}^A with A for either E, M, C or L compartments and Q_{loss}).

– The *KGE* (Gupta et al., 2009) consists of a diagonal decomposition of the *NSE* (Nash and Sutcliffe, 1970) to separate Pearson's correlation coefficient r_p , representation of bias β_{KGE} , and variability α_{KGE} . Thus, the *KGE* is comparable to multi-objective criteria for calibration purposes (Pechlivanidis et al., 2013). The sub-panel offers (i) a bi-plot of the three *KGE*'s components and (ii) a radar plot visualization of the *KGE*'s components, allowing to identify potential

205 to multi-objective criteria for calibration purpose (Pechlivanidis et al., 2013). The sub-panel offers (i) a bi-plot of the three *KGE*'s components and (ii) a radar plot visualization of the *KGE*'s components, allowing to identify potential counterbalancing errors according to these different components (Cinkus et al., 2023a). The two above-mentioned plots

also include the decomposition of the *KGENP* (Pool et al., 2018) in terms of Spearman's rank correlation coefficient r_s , representation of bias β_{KGENP} and non-parametric variability α_{KGENP} .

240 3.4 Dealing with uncertainties

Moges et al. (2021) summarize the various sources of uncertainties in hydrological models including structural and parametric 210 uncertainties as well as uncertainties related to input data and observations. The latter concern both the input (i.e. precipitation and evapotranspiration) and the output (i.e. discharge) of the modeled systems. Many references are devoted to the uncertainties related to input data and observations. As an example, Westerberg et al. (2020) include information about the discharge

245 uncertainty distribution in the objective function and perform better discharge simulation. Also, the precipitation error can be dependent on the data time step (McMillan et al., 2011) and could impact the hydrological model performance (Ficchi et al., 215 2016). Lumped parameter hydrological models generally consider meteorological time series representative of a whole catchment, which may require some pre-processing, particularly for snow processes since it can have a strong influence on flow dynamics. Thus, KarstMod includes variables related to both the snow routine (i.e. the redistributed precipitation time

a mis en forme : Espace Après : 12,95 pt, Interligne : Multiple 1,08 li

a mis en forme : Police : Cambria, Italique, Exposant

a mis en forme : Retrait : Gauche : -0,03 cm, Espace Après : 15,05 pt, Interligne : Multiple 1,08 li, Taquets de tabulation : 9,88 cm, Centré

a mis en forme : Gauche, Retrait : Gauche : 1,38 cm, Suspendu : 0,35 cm, Droite : 0 cm, Espace Après : 0 pt, Interligne : simple

a mis en forme : Espace Après : 10,6 pt

a mis en forme : Taquets de tabulation : 1,07 cm, Centré

a mis en forme : Police : 8,5 pt

a mis en forme : Police : 10 pt

a mis en forme : Police : 8,5 pt

229 series P_{sr}) and the PET routine (i.e. estimated potential evapotranspiration PET) in the parameter estimation procedure. This allows us to investigate the sensitivity of the flow simulation to these input data, when using snow and PET routines. Nonetheless, 220 KarstMod does not include features to investigate the impact of observation uncertainties on the parameter estimation.

As with many environmental problems, parameter estimation in rainfall-discharge modeling consists generally of ill-posed problems, i.e. the modeling encounters issues about the unicity, identifiability, and stability of the problem solution (Ebel and

225 Loague, 2006). As a consequence, several representations of the modeled catchment may be considered as equally acceptable

(Beven, 2006). Knoben et al. (2020) evaluate the performance of 36 daily lumped parameter models over 559 catchments and 225 show that between 1 and up to 28 models can show performance close to the model structure with the highest performance criteria. Such results are widely covered in catchment hydrology (Zhou et al., 2021; Pandi et al., 2021; Dakhlaoui and Djebbi, 2021; Darbandsari and Coulibaly, 2020; Gupta and Govindaraju, 2019) but still poorly investigated in karst hydrology. Indeed, 230 the structural uncertainty impacts on rainfall-discharge modeling in karst hydrology is not properly evaluated whereas many studies consider several hydrological model structures to include structural uncertainty in flow simulation (Hartmann et al.,

230 2012; Jiang et al., 2007; Jones et al., 2006; Sivelle et al., 2021). KarstMod includes more than 50 combinations of the various compartments as well as various compartments model (i.e. compartment with linear or non-linear discharge law and compartment with infinite characteristic time) and allows a quick implementation of the various model structures. The user can easily

235 manage to start the modeling with one single compartment and gradually move to a more complex model structure with up to 4 compartments, 5 fluxes connected to the spring, 4 internal fluxes, and 1 flux running out of the system.

235 Considering each model structure, parametric equifinality can be investigated using (i) dot plots of the values of the objective function against the parameter values, (ii) dot plots of the values of the performance criteria used to define the aggregated objective function, and (iii) the variance-based, first-order S_i and total S_{Ti} sensitivity indexes for the model parameters. Details concerning the computation of sensitivity indexes within KarstMod are given in Mazzilli et al. (2019, 2022).

4 Examples of application

240 To illustrate the KarstMod application and the use of the above-presented functionalities for the assessment of karst groundwater resources, we propose two case studies: (i) the Touvre karst system and (ii) the Lez karst system. Both karst systems consist of strategic freshwater resources for drinking water supply (DWS), for the city of Angoulême (western France) and Montpellier (southern France) respectively.

a mis en forme : Police :10 pt

a mis en forme : Retrait : Gauche : -0,01 cm, Première ligne : 0 cm

a mis en forme : Police :10 pt

a mis en forme : Police :8,5 pt

a mis en forme : Police :10 pt

a mis en forme : Police :8,5 pt, Français (France)

a mis en forme : Police :10 pt

a mis en forme : Retrait : Gauche : -0,03 cm, Suspendu : 0,87 cm, Droite : -0,03 cm, Espace Après : 0,15 pt, Interligne : Multiple 1,39 li

a mis en forme : Retrait : Gauche : -0,03 cm, Suspendu : 0,85 cm, Espace Après : 20,55 pt

a mis en forme : Police :10 pt

a mis en forme : Retrait : Gauche : -0,03 cm, Suspendu : 0,85 cm, Espace Après : 10,75 pt

4.1 The Touvre karst system (La Rochefoucauld)

²⁴⁵ The Touvre karst system is a karst system where the infiltration consists of (i) a delayed infiltration of effective rainfall on the karstic recharge area and (ii) a direct infiltration of surface water from the Tardoire, Bandiat, and Bonnieure rivers. The latter are surface stream flows within metamorphic rocks that partly infiltrate to subterranean at the contact with sedimentary formations, ²⁵⁰ mainly composed of Middle to Upper ~~Jurassic~~ Jurassic limestones. The springs of the Touvre, located 7 km east of Angoulême (western

France), have three main outlets (the Bouillant, the Dormant, and the Font de Lussac) and a secondary outlet (the Lèche) (Labat ²⁵⁰ et al., 2022). In the following, the discharge of the four outlets ~~are~~ is accumulated and named Touvre spring.

The Touvre karst system constitutes a strategic freshwater resource for the drinking water supply (DWS) of Angoulême, with around 110,000 inhabitants, but also contributes to the water supply for industry and agriculture. In 2015, there were 84 pumping

²⁵⁵ wells over the karstic impluvium of the Touvre karst system, and around 100 more in the Tardoire, Bandiat, and Bonnieure rivers catchment. Based on the data provided by the Adour-Garonne Water Agency, the annual groundwater

²⁵⁵ abstraction for agriculture represents 4.6 Mm³ whereas annual groundwater abstraction for DWS represents 1.1 Mm³ over the karstic impluvium of the Touvre karst system. On the three rivers catchment (out of the karstic impluvium), the annual groundwater abstraction represents 2.5 Mm³ for agriculture and 3.3 Mm³ for DWS, mainly through river intakes or alluvial groundwater

²⁶⁰ abstraction. The total annual volume of abstracted groundwater in the area represents around 5 % of the annual volume of transit at the Touvre ~~spring~~ Spring. This is quite low compared with karst aquifers in France exploited for their groundwater resource

²⁶⁰ resources, such as the Lez spring (Jourde et al., 2014) and the Oeillal's spring karst catchment (Sivelle et al., 2021), where the annual groundwater abstraction volume represents respectively 50 % and 15 % of the annual volume of transit at the spring. Therefore, the Touvre karst system seems not to be over-exploited at the moment but the impact of groundwater abstraction should be ²⁶⁵ addressed in the context of global change to ensure ~~a~~ sustainable management of this strategic ~~fresh~~ freshwater resource.

The area is characterized by an ocean-influenced climate with a mean annual precipitation of around 800 mm/year distributed ²⁶⁵ over an average of 255 rainy days. The estimation is performed with Thiessen polygon methods based on eleven meteorological stations over the area (Labat et al., 2022). The mean annual potential evapotranspiration is around 770 mm/year according to the Penman-Monteith estimation provided by the French meteorological survey (Météo-France). The Touvre daily spring ²⁷⁰ discharge shows a significant variability ranging from 3 m³/s to 49 m³/s with a coefficient of variation around 0.46 (Figure 4b).

The surface stream flow rates for the Bonnieure, Bandiat, and Tardoire rivers are concentrated within the autumn and winter

a mis en forme : Retrait : Gauche : -0,03 cm, Première ligne : 0,85 cm

a mis en forme : Police :10 pt

a mis en forme : Police :8,5 pt

a mis en forme : Police :10 pt

a mis en forme : Retrait : Gauche : -0,03 cm, Suspendu : 0,85 cm

a mis en forme : Police :8,5 pt

a mis en forme : Police :10 pt

270 periods. During the summer period, the discharge in the three rivers are very low (Figure 4c). The more significant groundwater abstraction is performed during the summer period, while the Touvre spring discharge reaches its lowest values within the late summer and early autumn periods (Figure 4, c and d).

275 Figure 3 shows the model structure for the Touvre karst system that consists of three compartments organized in two levels (Labat et al., 2022). The upper level corresponds to reservoir E and represents both the unsaturated part of the system and 275 a temporary aquifer. This reservoir is connected with the two reservoirs of the lower level: C (Conduit) and M (Matrix) representative of quick and slow flow dynamics respectively. The upper level of the model structure is affected by precipitation

280 P and potential evapotranspiration PET while the lower level of the model structure is affected by (i) groundwater abstraction and (ii) sinking river stream-flow from the surface to underground. Figure 4 shows the various time series required for the hydrological modeling of the Touvre karst system. The methodology for daily time series preparation given in Labat et al.

280 (2022) allows us to account for the influence of groundwater abstraction on the transmissive or capacitive part of the karst aquifer as well as the influence of concentrated and diffuse infiltration of the surface river stream-flow.

a mis en forme : Police :8,5 pt
a mis en forme : Retrait : Gauche : -0,03 cm, Suspendu : 0,87 cm, Droite : -0,03 cm, Espace Après : 0,15 pt, Interligne : Multiple 1,39 li

a mis en forme : Police :8,5 pt

a mis en forme : Police :10 pt

a mis en forme : Police :8,5 pt

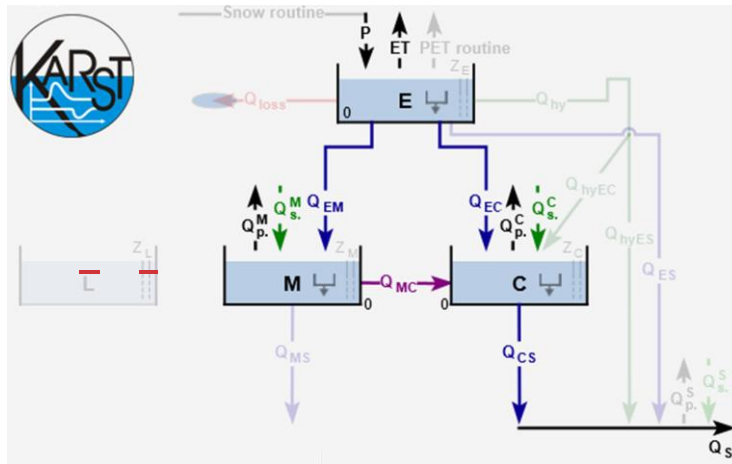


Figure 3. Screenshot of KarstMod with a focus on the panel "Model structure" for the Touvre karst system. The solid lines correspond to the activated fluxes whereas the faded color lines are not activated. Q_p^M and Q_p^C stand for groundwater abstraction that affects compartments M and C respectively while $Q_{s.p}^M$ and $Q_{s.p}^C$ stand for sinking flow that affects compartments M and C respectively.

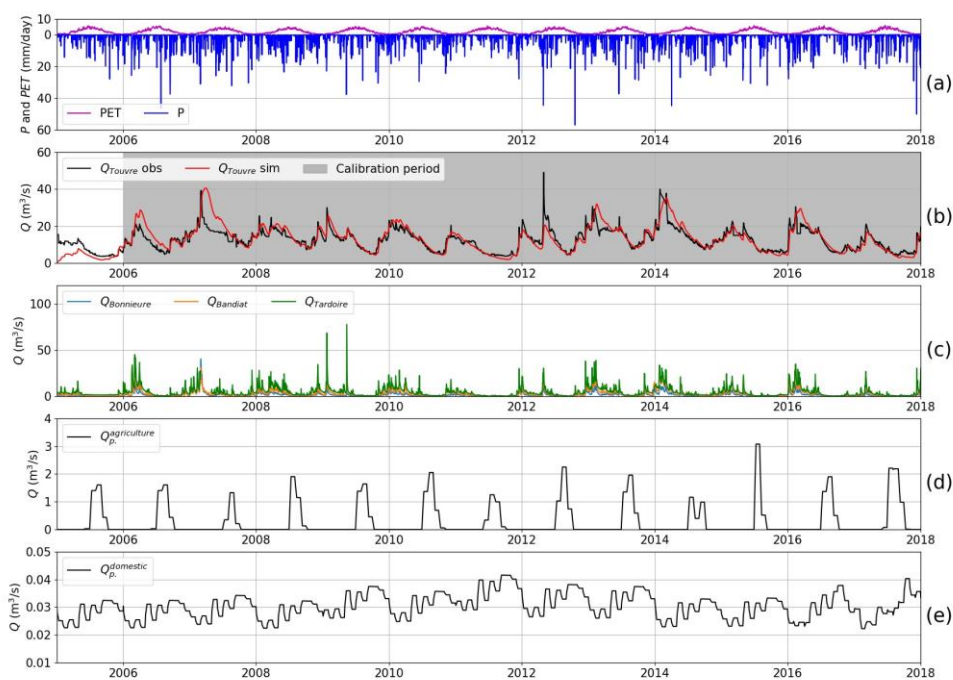


Figure 4. Daily time series for the Touvre system: a) precipitation (P) and potential evapotranspiration (PET), b) observed and simulated karst spring discharge ($Q_{Touvre\ obs}$ and $Q_{Touvre\ sim}$), c) observed river streamflow discharge ($Q_{Bonnieure}$, $Q_{Bandiat}$, $Q_{Tardoire}$), d) and e) groundwater abstraction discharge ($Q_{agriculture\ p.}$, $Q_{domestic\ p.}$).

The objective of the hydrological modeling is to assess the impact of groundwater abstraction on spring discharge, and more particularly during low flow periods (Labat et al., 2022). So, the calibration is performed according to the *KGENP* that improves the simulations during mean and low-flow conditions using the Spearman rank correlation due to its insensitivity to

extreme values (Pool et al., 2018). The sampling procedure is set up to find $n_{obj} = 5000$ simulations with *KGENP* greater than 0.9. Afterwards, the model is evaluated using the various features proposed in *KarstMod* (Figure 5). The diagnostic efficiency plot (Figure 5a) testifies of several elements: (i) the model seems to slightly overestimate high flow and underestimate low

a mis en forme : Police :8,5 pt, Français (France)

296 flow, (ii) the timing error is about 0.9, testifying of suitable flow dynamics in the model, (iii) low flow periods contribute more to the model errors, and (iv) there is no offset in the simulated spring hydrograph. The radar chart (Figure 5b) shows a good 290 equilibrium between the various objective functions whose values are greater than 0.8, excepted for the *NSE* criteria (*NSE* = -0.75). It is the consequence of the design of these criteria that tends to outweigh the errors during floods. Here the *NSE* value is still greater than 0.7 and testifies of a "very good" fit according to Moriasi et al. (2007). Finally, the decomposition of the 295 *KGE* (Figure 5 c and d) shows $r_p = 0.91$, $\alpha = 1.15$ and $\beta = 1.02$ testifying of accurate dynamics and low bias, but slightly too high variability.

a mis en forme : Police :10 pt

a mis en forme : Retrait : Gauche : -0,01 cm, Première ligne : 0 cm

a mis en forme : Police :10 pt

a mis en forme : Retrait : Gauche : 0 cm, Première ligne : 0 cm

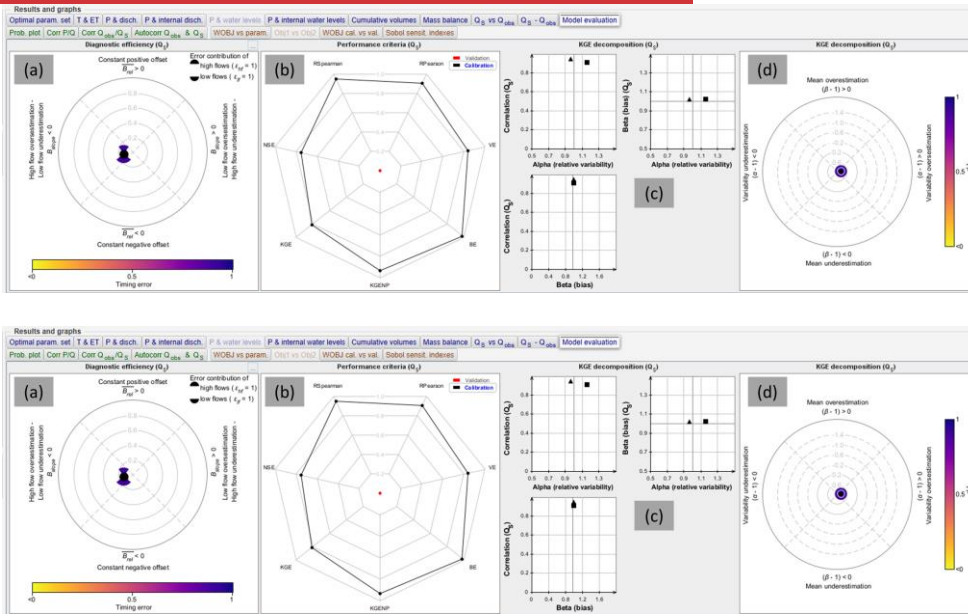


Figure 5. Screenshot of KarstMod with a focus on the sub-panel "Model evaluation". Application for the model evaluation on the Touvre system: (a) diagnostic efficiency plot (Schwemmler et al., 2021), (b) radar chart of the objective functions, (c) bi-plot of the *KGE*'s (square) and *KGENP*'s (triangle) components, and (d) radar chart of the *KGE*'s components.

a mis en forme : Espace Après : 15,5 pt

295 4.2 The Lez spring

The Lez spring (southern France) consists of the main outlet of a karst system encompassed in the North Montpellieran Garrigue hydrogeological unit delimited to the west by the Hérault ~~river~~River, and to the north and east by the Vidourle ~~river~~River. The

~~300~~ geology in the area corresponds to the Upper Jurassic layers separated by the Corconne-Matelle fault (oriented N30°), leading to two main compartments in the aquifer (Bérard, 1983; Clauzon et al., 2020). The karst aquifer is unconfined in the

~~300~~ western compartment and is locally confined in the eastern compartment. The Lez ~~spring~~Spring is located about 15 km north of

Montpellier. It is of Vaclousian-type with an overflow level at 65 m a.s.l. and a maximum daily discharge of approximately 15 m³ s⁻¹. The area is characterized by a typical Mediterranean climate with dry summers and rainy autumns. Over the ~~2009-2019~~~~2009~~2019 period,

~~305~~ the mean annual precipitation is around 900 mm/year distributed over an average of 133 rainy days (estimation with Thiessen polygon methods based on four meteorological stations over the area: Prades-le-Lez, Saint-Martin-de-Londres,

~~305~~ Sauteyrargues, and Valflaunès), a mean annual potential evapotranspiration is around 900 mm/year according to the estimation based on Oudin's formula with the temperature measured at Prades le Lez station while the ~~mean~~real annual evapotranspiration is around 450 mm/year (eddy covariance flux-station of Puéchabon).

~~310~~ Since 1854, the Lez spring supplies the drinking water to Montpellier city and the surroundings. It currently constitutes the main ~~fresh-water~~freshwater resource for around 350,000 people in the area. The present water management scheme allows pumping at

~~310~~ higher rates than the natural spring discharge during low flow periods, while supplying a minimum discharge rate (~ 230 l/s) into the Lez ~~river~~River to ensure ecological flow downstream, and reducing flood hazards via rainfall storage in autumn (Avias, 1995; Jourde et al., 2014). The pumping plant was built in 1982 with four deep wells drilled to intercept the karst conduit feeding the

~~315~~ spring, 48 m below the overflow level of the spring. Pumping in these wells allows up to 1800 l/s to be withdrawn under low flow periods (with an authorized maximum drawdown of 30 m), while the average annual pumping flow rate is about

~~315~~ 1010 l/s (over the 2008-2019 period). Due to the pumping management of the aquifer, which supplies about 30 to 35 Mm³ of water per year to the metropolitan area of Montpellier, the discharge at the Lez spring is often low or nil. Discharge is also measured downstream (Lavalette gauging station) where the measured discharge corresponds to the Lez spring discharge and the main tributaries (Lirou and Terrieu streams) which flow essentially after intense Mediterranean rainfall events. As suggested in Cousquer and Jourde (2022), the surface water discharge, denoted Q_{DSS} , can be estimated as the difference between the total discharge in Lavalette and the Lez spring discharge.

In the present context of global change, Mediterranean karst systems already show significant decrease in spring discharge

a mis en forme : Taquets de tabulation : Pas à 1,07 cm

a mis en forme : Police :10 pt

a mis en forme : Police :8,5 pt

a mis en forme : Police :10 pt

a mis en forme : Police :8,5 pt

a mis en forme : Police :8,5 pt

a mis en forme : Police :10 pt

a mis en forme : Police :8,5 pt

a mis en forme : Retrait : Gauche : -0,01 cm, Première ligne : 0 cm

a mis en forme : Espace Après : 3,85 pt

320 (Hartmann et al., 2012; Fiorillo et al., 2012; Smiatek et al., 2013; Doummar et al., 2018b; Nerantzaki and Nikolaidis, 2020; Dubois et al., 2020) which could be aggravated with groundwater abstraction (Sivelle et al., 2021). The Lez spring is strongly exposed to global change impact: (i) the Mediterranean area is identified as a climate change hot-spot (Diffenbaugh and

325 Giorgi, 2012) where the projected warming spans 1.8–8.4 °C according to CMIP6 and 1.2–6.6 °C according to CMIP5 during the summer period (Cos et al., 2022), and (ii) the water management scheme will have to adapt to the future need in drinking water

a mis en forme : Police :8,5 pt

325 for the growing population in the area as well as changes in the ~~fresh water~~ freshwater consumption practice (e.g. water use restriction order). Therefore, a sustainable water management plan for the Lez ~~spring~~ Spring requires a good appreciation of the hydrological functioning as well as the operational hydrological model to properly address ~~impacts~~ impact studies. In this framework, KarstMod

a mis en forme : Police :10 pt

330 allows for choosing and calibrating a suitable model structure. This constitutes ~~a~~ the first step for a global change impact study that requires prediction tools to simulate the aquifer response to various external ~~forcing~~ forces.

a mis en forme : Police :8,5 pt

330 Figure 6 shows the model structure for the Lez karst catchment (Mazzilli et al., 2011) that consists of three compartments organized in two levels. The upper level corresponds to compartment E and represents the unsaturated part of the system, including a soil water holding capacity E_{min} and a discharge lost from the compartment Q_{loss} . The compartment E is exposed

335 to precipitation P and evapotranspiration ET and discharge towards the lower level of the model structure starts when the water level exceeds the water holding E_{min} . The lower level consists of two inter-connected compartments M and C allowing

a mis en forme : Police :8,5 pt

335 to ~~reproduce~~ reproduction of the lateral exchanges, denoted Q_{MC} , between the transmissive function (compartment C) and the capacitive function (compartment M) of the karst aquifer. Both M and C compartments are considered bottomless, allowing to reproduce ~~period~~ periods of non-overflow at the Lez spring when the mean water level in the aquifer stands below 65 m a.s.l., mainly during

a mis en forme : Police :10 pt

340 summer periods due to pumping in the karst conduit. Figures 7a and 7b show the various daily time series required for the hydrological modeling of the Lez karst system (i.e. P , ET and Q_{pump}).

a mis en forme : Police :8,5 pt

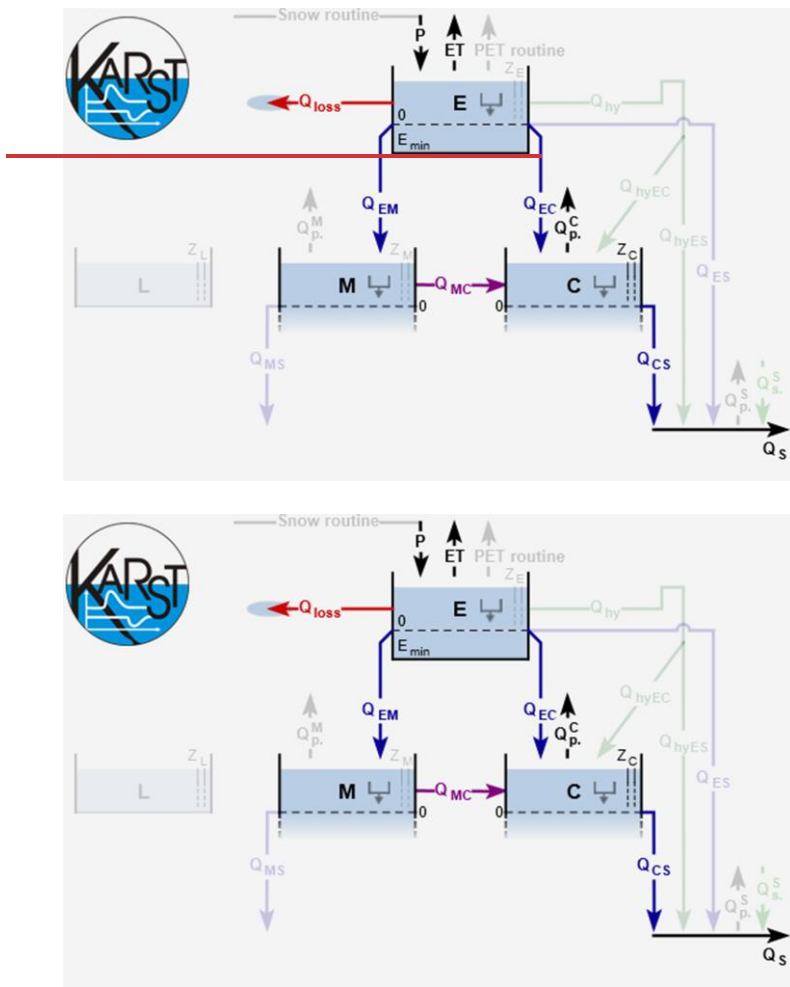
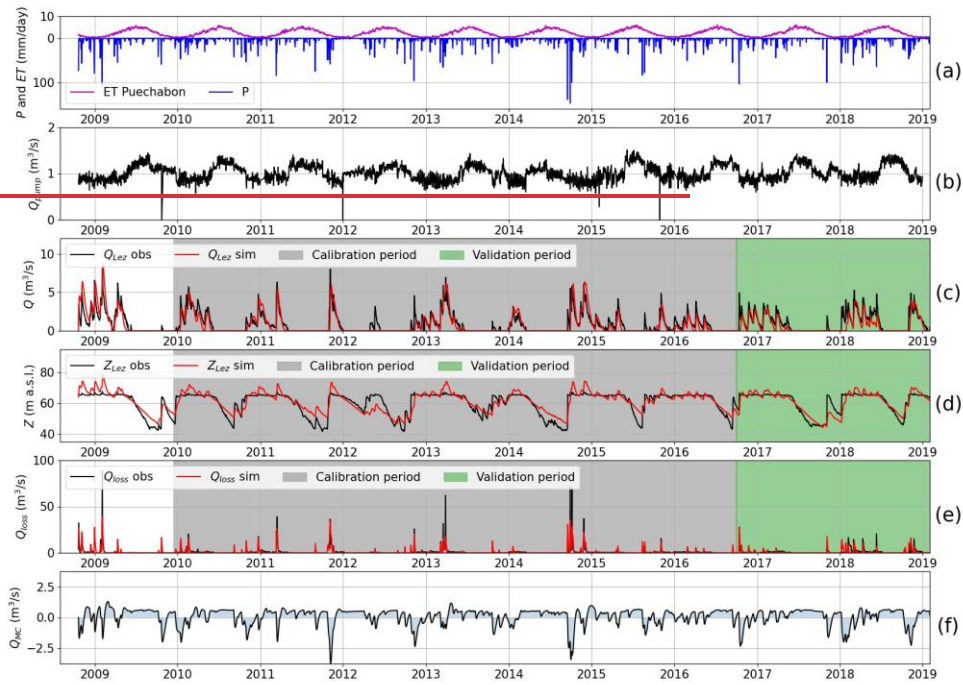


Figure 6. Screenshot of KarstMod with a focus on the panel "Model structure" for the Lez karst system. The solid lines correspond to the

the activated fluxes whereas the faded color lines are not activated. Q_{loss} stands for the surface water discharge from the epikarst compartment, Q_p^C stands for groundwater abstraction that affects compartments C while Z_C stands for piezometric head measurements considered as representative of the compartment C.



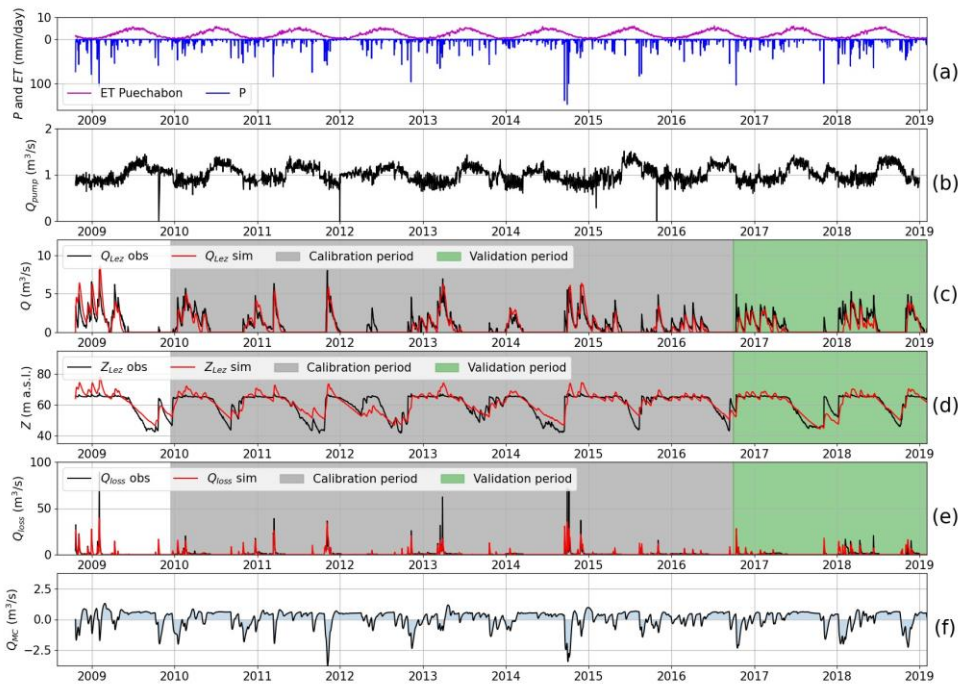


Figure 7. Daily time series for the Lez system: a) precipitations (P) and evapotranspiration (ET), b) groundwater abstraction (Q_{pump}), c) observed and simulated karst spring discharge ($Q_{Lez\ obs}$ and $Q_{Lez\ sim}$), d) observed and simulated piezometric head ($Z_{Lez\ obs}$ and $Z_{Lez\ sim}$), e) surface water discharge (Q_{loss}) and f) simulated exchanges fluxes between compartment M and C (Q_{Mc}).

a mis en forme : Espace Après : 15,15 pt

340 The available hydrological observations for model calibration consist of spring discharge Q_s , piezometric head measurement Z_C at the Lez spring, and surface water discharge from secondary outlets and intermittent springs Q_{loss} (Figure 7, c, d, and e).

The surface water discharge is estimated as the difference in discharge measured at the Lavalette station (15 km downstream 345 of the Lez spring) and the discharge measured at the Lez spring, as proposed by Cousquer and Jourde (2022). Therefore, Q_{loss} includes all the water loss from the epikarst within several seasonal overflowing springs (i.e. Lirou spring, Restinclière spring

345 and Fleurette spring). KarstMod allows ~~to easily handle with~~ for easy handling of the various parameter ~~estimation~~ estimations depending on the considered hydrological observations (i.e. spring discharge, piezometric head measurement, and surface discharge from the epikarst). The sampling procedure is set up to find $n_{obj} = 5000$ simulations with an aggregated objective function Φ greater than 0.6. As 350 suggested by Cousquer and Jourde (2022), using complementary hydrological observations in addition to the spring discharge allows for to reduce the parametric uncertainties in the modeling of the Lez spring discharge. Therefore, using a multi-objective 350 calibration procedure implemented in KarstMod, the objective function is ~~built~~ built such as:

$$\Phi = \frac{1}{3} \times NSE(Q_s) + \frac{1}{3} \times NSE(Z_C) + \frac{1}{3} \times NSE(Q_{loss}) \quad \Phi = \frac{1}{3} \times NSE(Q_s) + \frac{1}{3} \times NSE(Z_C) + \frac{1}{3} \times NSE(Q_{loss}) \quad (4)$$

The calibration procedure leads to an optimal $\Phi = 0.65$ decomposed such as $\phi_{Q_s} = 0.70$, $\phi_{Z_C} = 0.57$ and $\phi_{Q_{loss}} = 0.70$ 355 within the calibration period. Model performance evaluation on the validation period shows suitable model performance for both spring discharge and piezometric with $\phi_{Q_s} = 0.54$ and $\phi_{Z_C} = 0.79$, but poor model performance according to the surface

355 water discharge with $\phi_{Q_{loss}} = 0.36$. Afterwards, the results can be evaluated using the various features proposed in KarstMod (Figure 8). The results show higher model performances for Q_s and Z_C than for Q_{loss} . The model performance appears quite ~~satisfactorily~~ satisfactory concerning the variable of interest to assess the impact of the water management scheme on the groundwater 360 resources within the Lez aquifer.

The simulated exchange fluxes between ~~compartment~~ compartments M and C (Figure 7f) show consistent dynamics with the observations.

360 Indeed, during periods of high flow, the exchange fluxes are oriented from ~~the~~ compartment C to compartment M (i.e. $Q_{MC} < 0$). Significant precipitation events lead to rapid rises in the piezometric head, saturation of the transmissive part of the aquifer, and finally the establishment of overflow at the Lez spring (i.e. $Q_s > 0$) as well as the overflowing springs (i.e. $Q_{loss} > 0$).

365 Conversely, during the periods of low piezometric head (i.e. both Q_s and Q_{loss} are nil), the simulated exchange fluxes are oriented from compartment M to compartment C (i.e. $Q_{MC} > 0$). Such flow exchanges between capacitive and transmissive ~~part parts~~ of karst aquifers ~~has~~ have been evidenced using KarstMod on other karst environment (Sivelle et al., 2019; Duran et al., 2020; Frank et al., 2021; Labat et al., 2022).

a mis en forme : Police :10 pt

a mis en forme : Retrait : Gauche : -0,01 cm, Première ligne : 0 cm

a mis en forme : Police :8,5 pt

a mis en forme : Police :8,5 pt

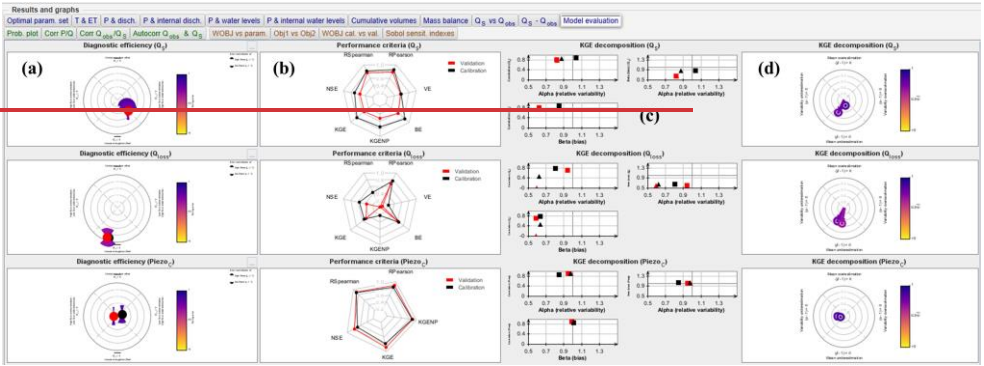
a mis en forme : Police :10 pt

a mis en forme : Retrait : Gauche : -0,01 cm, Première ligne : 0 cm

a mis en forme : Police :8,5 pt

a mis en forme : Police :10 pt

a mis en forme : Police :8,5 pt



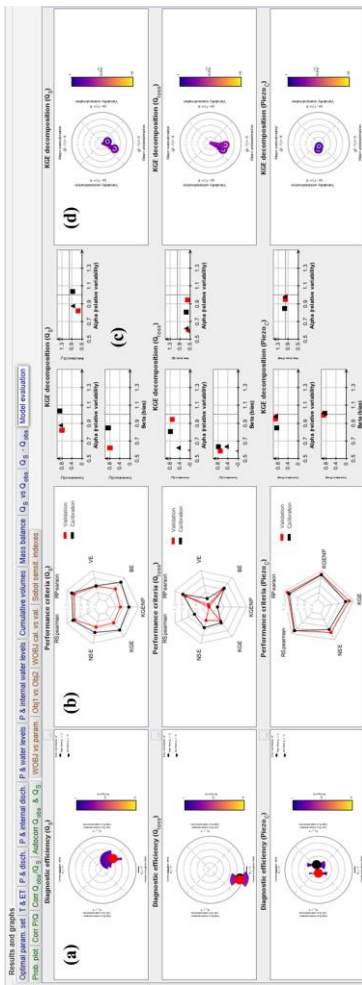


Figure 8. Screenshot of KarstMod with a focus on the sub-panel "Model evaluation". Application for the model evaluation on the Lez system. The panel is composed such as (i) each row corresponds to the variable for calibration (Q_s , Q_{loss} and $Piezo_c$) and (ii) each column

a mis en forme : Espace Après : 0 pt

corresponds to (a) diagnostic efficiency plot, (b) radar plots, one should note that *VE* and *BE* are not computed according to the piezometric time series, (c) decomposition of *KGE* (square) and *KGENP* (triangle) and (d) radar plot of the *KGE* decomposition.

5 Conclusions

370 KarstMod consists ~~in~~of a useful tool for the assessment of karst groundwater variability and sensitivity to anthropogenic pressures (e.g. groundwater abstraction). This tool is devoted to ~~promote~~promoting good practices in hydrological modeling for learning and

375 occasional users. KarstMod requires no programming skills and offers a user-friendly interface allowing any user to easily handle hydrological modeling. As a first step, KarstMod can be used to explore the ability of conceptual representations to explain observations such as discharge or piezometric heads in karst systems. ~~A more~~More advanced use of KarstMod is also possible as it provides a complete framework for (i) primary analysis of the data, (ii) comparison of various model structures, (iii) evaluation of the hydrological model performance as well as (iv) first assessment of parametric uncertainties. The research

375 community increasingly uses KarstMod to address various challenges in karst hydrology, from understanding hydrological processes to practical applications such as evaluation of groundwater management ~~plans~~plans, or even assessment of the impact of groundwater abstraction and climate changes on karst groundwater resources.

380 Future developments of KarstMod might include: (i) the consideration of ~~land cover land use (LCLU) to consider~~ the spatial heterogeneity in recharge processes which is essential when considering snowmelt as well as land cover (Sivelle et al., 2022a), (ii) the simulation of electrical conductivity (Chang et al., 2021),

385 major ions concentration (Hartmann et al., 2013) or natural tracer such as air excess (Sivelle et al., 2022b), and (iii) the assessment of structural uncertainty (Cousquer et al., 2022). KarstMod should tend toward an ~~open source~~opensource research software to avoid duplication of efforts in karst hydrological modeling. Also, a Python version is required

385 for a better connection with an additional framework for sensitivity analysis such as SAFE toolbox (Pianosi et al., 2015) and for model calibration ~~procedure~~procedures such as particle swarm optimization (Eberhart and Kennedy, 1995; Lee, 2014). Finally, the development of the

385 KarstMod modeling platform will benefit better transparency and repeatability with an open-source approach, as observed on other numerical tools (Pianosi et al., 2020).

Appendix A: Snow routine

390 Figure A1 shows the general workflow implemented in the snow routine. P_{sr}^* (liquid water leaving the routine) is estimated for each time step t based on the precipitation P and air temperature T time series for each sub-catchment. The total snow routine output P_{sr} is calculated as a weighted sum of P_{sr}^* time series:

a mis en forme : Police :10 pt

a mis en forme : Police :8,5 pt

a mis en forme : Police :10 pt

a mis en forme : Police :10 pt

a mis en forme : Police :8,5 pt

a mis en forme : Police :10 pt

a mis en forme : Espace Après : 19,45 pt

a mis en forme : Espace Après : 15,25 pt

a mis en forme : Retrait : Gauche : -0,03 cm, Suspendu : 0,85 cm, Espace Après : 16,9 pt

a mis en forme : Police :10 pt

$$P_{sr} = \sum_i^N P_{sr_i} \times p_i \quad (A1)$$

where p_i is the proportion of the sub-catchment i regarding the complete catchment area such as $\sum p_i = 1$, and N is total number of sub-catchments.

The snow routine requires four parameters, whose values are the same for all sub-catchments: the snowmelt temperature threshold T_s [$^{\circ}\text{C}$], the melt factor MF [$\text{L T}^{-1} \cdot \text{C}^{-1}$], the refreezing factor CFR [-], and the water holding capacity of snow CWH [-]. The snow routine allows estimating P_{sr} according to the algorithm A1.

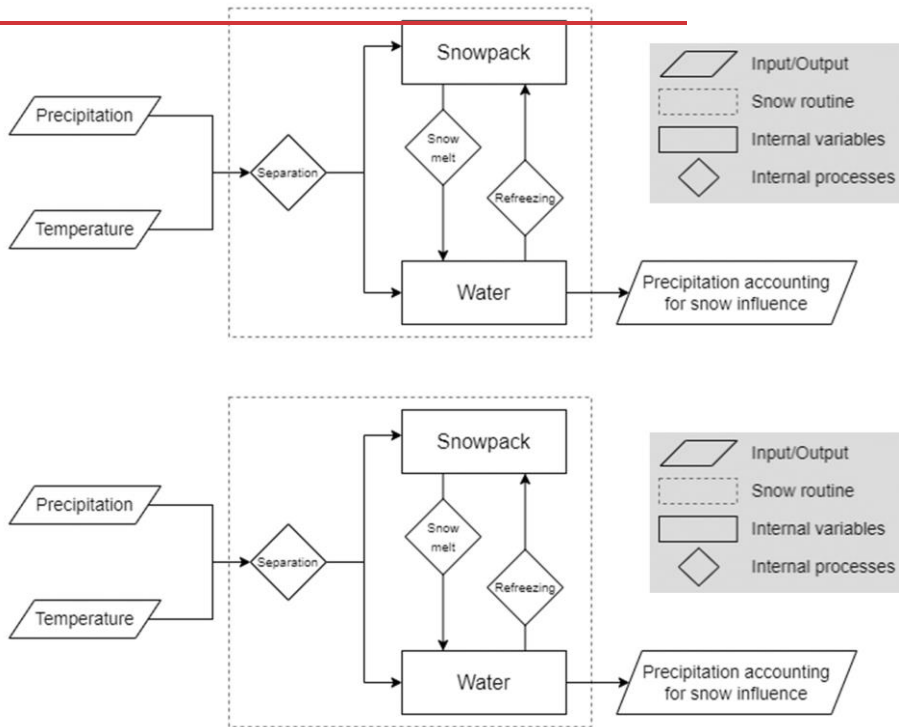


Figure A1. Snow routine workflow.

a mis en forme : Retrait : Gauche : -0,03 cm, Première ligne : 1,2 cm, Espace Après : 0 pt, Interligne : simple

a mis en forme : Police : 10 pt

a mis en forme : Retrait : Gauche : 0,85 cm, Première ligne : 0,35 cm, Espace Après : 1,4 pt

a mis en forme : Espace Après : 13,25 pt

Algorithm A1 Estimating Ps_r^* in sub-catchment

With Ps_r^* = water leaving the routine/recharge to the soil (mm/dt), T_a = active temperature for snowmelt ($^{\circ}$ C), T_n = active temperature for refreezing ($^{\circ}$ C), m = snow melt (mm/dt), rfz = refreezing (mm/dt), v = solid component of snowpack depth (mm), vl = liquid component of snowpack depth (mm), and dt = temporal resolution. for $t=1$ to t_{max} do

```
 $m[t] = \min(MF \times T_a[t], v[t])$  with  $T_a[t] = T[t] - T_s$   
 $rfz[t] = \min(CFR \times MF \times T_n[t], vl[t])$  with  $T_n[t] = T_s - T[t]$   
 $v[t + dt] = v[t] - m[t] + snow[t] + rfz[t]$   
if  $vl[t + dt] > CWH \times v[t + dt]$  then  
|  $Ps_r^*[t] = vl[t + dt] - CWH \times v[t + dt]$   
|  $vl[t + dt] = CWH \times v[t + dt]$   
else  
|  $Ps_r^*[t] = 0$   
end  
end
```

```
 $m[t] = \min(MF \times T_a[t], v[t])$  with  $T_a[t] = T[t] - T_s$   
 $rfz[t] = \min(CFR \times MF \times T_n[t], vl[t])$  with  $T_n[t] = T_s - T[t]$   
 $v[t + dt] = v[t] - m[t] + snow[t] + rfz[t]$   
if  $vl[t + dt] > CWH \times v[t + dt]$  then  
|  $Ps_r^*[t] = vl[t + dt] - CWH \times v[t + dt]$   
|  $vl[t + dt] = CWH \times v[t + dt]$   
else  
|  $Ps_r^*[t] = 0$   
end  
end
```

a mis en forme : Espace Après : 1,65 pt

400 vatory network (SNO KARST) initiative from the INSU/CNRS. The platform can be downloaded here: <https://sokarst.org/en/software-en/karstmod-en/>

400 *Author contributions*. V. Sivelle: methodology, software, writing—original draft. G. Cinkus: methodology, software, writing—review, and editing. N. Mazzilli: methodology, software, project administration, writing—review and editing. H. Jourde: methodology, software, project administration, funding acquisition, writing—review and editing. D. Labat: methodology, software, writing—review, and editing. B. Arfib:

405 methodology, software, writing—review and editing. N. Massei: methodology, software, writing—review and editing. Y. Cousquer: writing—review and editing. D. Bertin: methodology, software, writing—review, and editing.

405 *Competing interests*. The authors declare no competing interest.

Acknowledgements. This platform is developed within the framework of the KARST observatory network (SNO KARST) initiative from the INSU/CNRS (France), which aims to strengthen knowledge-sharing and promote crossdisciplinary research on karst systems at the national 410 scale. This work, as well as V. ~~Sivelle~~Sivelle's post-doctoral position, was supported by the European Commission through the Partnership for Research and Innovation in the Mediterranean Area (PRIMA) program under Horizon 2020 (KARMA project, grant agreement number ~~410~~ 01DH19022A).

a mis en forme : Retrait : Gauche : 0 cm, Suspendu : 0,85 cm, Espace Après : 0 pt, Interligne : simple

a mis en forme : Police :8,5 pt

a mis en forme : Espace Après : 34,6 pt, Interligne : Multiple 1,41 li

a mis en forme : Retrait : Gauche : 0,84 cm

a mis en forme : Police :8,5 pt

a mis en forme : Retrait : Gauche : 0 cm, Suspendu : 0,85 cm, Interligne : Multiple 1,41 li

References

- Andréassian, V.: On the (im)possible validation of hydrogeological models, *Comptes-Rendus-Géoscience*, 355, 1–9, 415 <https://doi.org/10.5802/crgeos.142>, 2023.
- Avias, J. V.: Gestion active de l'exurgence karstique de la Source du Lez (Hérault, France) 1957-1994, *Hydrogéologie (Orléans)*, pp. 113–127, <http://pascal-francis.inist.fr/vibad/index.php?action=getRecordDetail&idt=6307091>, 1995.
- Bailly-Comte, V., Borrell-Estupina, V., Jourde, H., and Pistre, S.: A conceptual semidistributed model of the Coulazou River as a tool for assessing surface water-karst groundwater interactions during flood in Mediterranean ephemeral rivers, *Water Resources Research*, 48, 420 <https://doi.org/10.1029/2010WR010072>, eprint: <https://onlinelibrary.wiley.com/doi/pdf/10.1029/2010WR010072.2012>.
- Bennett, N. D., Croke, B. F., Guariso, G., Guillaume, J. H., Hamilton, S. H., Jakeman, A. J., Marsili-Libelli, S., Newham, L. T., Norton, J. P., Perrin, C., Pierce, S. A., Robson, B., Seppelt, R., Voinov, A. A., Fath, B. D., and Andréassian, V.: Characterising performance of environmental models, *Environmental Modelling & Software*, 40, 1–20, <https://doi.org/10.1016/j.envsoft.2012.09.011>, 2013.
- Bergström, S.: The HBV model - its structure and applications., <https://www.smhi.se/en/publications/429425-the-hbv-model-its-structure-and-applications-1.83591>, 1992.
- Beven, K.: On explanatory depth and predictive power, *Hydrological Processes*, 15, 3069–3072, <https://doi.org/10.1002/hyp.500>, eprint: <https://onlinelibrary.wiley.com/doi/pdf/10.1002/hyp.500>, 2001.
- Beven, K.: A manifesto for the equifinality thesis, *Journal of Hydrology*, 320, 18–36, <https://doi.org/10.1016/j.jhydrol.2005.07.007>, 2006.
- Bierkens, M. F. P. and Wada, Y.: Non-renewable groundwater use and groundwater depletion: a review, *Environmental Research Letters*, 14, 425–425 <https://doi.org/10.1088/1748-9326/ab1a5f>, publisher: IOP Publishing, 2019.
- Bittner, D., Narany, T. S., Kohl, B., Disse, M., and Chiogna, G.: Modeling the hydrological impact of land use change in a dolomite-dominated karst system, *Journal of Hydrology*, 567, 267–279, <https://doi.org/10.1016/j.jhydrol.2018.10.017>, 2018.
- Bittner, D., Richieri, B., and Chiogna, G.: Unraveling the time-dependent relevance of input model uncertainties for a lumped hydrologic model of a pre-alpine karst system, *Hydrogeology Journal*, <https://doi.org/10.1007/s10040-021-02377-1>, 2021.
- Blöschl, G. and Sivapalan, M.: Scale issues in hydrological modelling: A review, *Hydrological Processes*, 9, 251–290, <https://doi.org/10.1002/hyp.3360090305>, 1995.
- Blöschl, G., Bierkens, M. F., Chambel, A., Cudennec, C., Destouni, G., Fiori, A., Kirchner, J. W., McDonnell, J. J., Savenije, H. H., Sivapalan, M., Stumpp, C., Toth, E., Volpi, E., Carr, G., Lupton, C., Salinas, J., Széles, B., Viglione, A., Aksoy, H., Allen, S. T., Amin, A., Andréassian, V., Arheimer, B., Aryal, S. K., Baker, V., Bardsley, E., Barendrecht, M. H., Bartosova, A., Batelaan, O., Berghuijs, W. R., Beven, K., Blume, T., Bogaard, T., Borges de Amorim, P., Böttcher, M. E., Boulet, G., Breinl, K., Brilly, M., Brocca, L., Buytaert, W., Castellarin, A., Castelletti, A., Chen, X., Chen, Y., Chen, Y., Chiffliard, P., Claps, P., Clark, M. P., Collins, A. L., Croke, B., Dathe, A., David, P. C., de Barros, F. P. J., de Rooij, G., Di Baldassarre, G., Driscoll, J. M., Duethmann, D., Dwivedi, R., Eis, E., Farmer, W. H., Feiccabrino, J., Ferguson, G., Ferrari, E., Ferraris, S., Ferschi, B., Finger, D., Foglia, L., Fowler, K., Gartsman, B., Gascoïn, S., Gaume, E., Gelfan, A., Geris, J., Gharari, S., Gleeson, T., Glendell, M., Gonzalez Bevacqua, A., González-Dugo, M. P., Grimaldi, S., Gupta, A. B.,

a mis en forme : Retrait : Gauche : 0 cm, Première ligne : 0,85 cm, Espace Après : 0 pt, Interligne : Multiple

a mis en forme : Police : 9 pt, Français (France)

a mis en forme : Retrait : Gauche : 0,83 cm, Suspensé : 0,35 cm

a mis en forme : Retrait : Gauche : 0 cm, Première ligne : 0,85 cm

a mis en forme : Taquets de tabulation : 1,38 cm, Centré

a mis en forme : Espace Après : 4,5 pt

a mis en forme : Espace Après : 0 pt, Interligne : Multiple 1,4 li

a mis en forme : Retrait : Gauche : 1,22 cm, Espace Après : 3,4 pt, Taquets de tabulation : Pas à 18,55 cm

a mis en forme : Espace Après : 4,25 pt

a mis en forme : Retrait : Gauche : 0 cm, Espace Après : 3,5 pt, Taquets de tabulation : 18,55 cm, Droite

- 440 — Guse, B., Han, D., Hannah, D., Harpold, A., Haun, S., Heal, K., Helfricht, K., Herrnegger, M., Hipsey, M., Hlaváčiková, H., Hohmann, C., Holko, L., Hopkinson, C., Hrachowitz, M., Illangasekare, T. H., Inam, A., Innocente, C., Istanbuluoglu, E., Jarihani, B., Kalantari, C., Kalvans, A., Khanal, S., Khatami, S., Kiesel, J., Kirkby, M., Knoben, W., Kochanek, K., Kohnová, S., Kolechkina, A., Krause, S., Kreamer, D., Kreibich, H., Kunstmann, H., Lange, H., Liberato, M. L. R., Lindquist, E., Link, T., Liu, J., Loucks, D. P., Luce, C., Mahé, G., Makarieva, O., Malard, J., Mashtayeva, S., Maskey, S., Mas-Pla, J., Mavrova-Guirguinova, M., Mazzoleni, M., Mernild, S., Misstear, S. M., Stein, L., Steinsland, I., Strasser, U., Su, B., Szolgay, J., Tarboton, D., Tauro, F., Thirel, G., Tian, F., Tong, R., Tussupova, K., 445 — B. D., Montanari, A., Müller-Thomy, H., Nabizadeh, A., Nardi, F., Neale, C., Nesterova, N., Nurtaev, B., Odongo, V. O., Panda, S., Pande, S., Pang, Z., Papacharalampous, G., Perrin, C., Pfister, L., Pimentel, R., Polo, M. J., Post, D., Prieto Sierra, C., Ramos, M.-H., Renner, 450 — M., Reynolds, J. E., Ridolfi, E., Rigon, R., Riva, M., Robertson, D. E., Rosso, R., Roy, T., Sá, J. H., Salvadori, G., Sandells, M., Schaeffli, B., Schumann, A., Scolobig, A., Seibert, J., Servat, E., Shafiei, M., Sharma, A., Sidibe, M., Sidle, R. C., Skaugen, T., Smith, H., Spiessl, S. M., Stein, L., Steinsland, I., Strasser, U., Su, B., Szolgay, J., Tarboton, D., Tauro, F., Thirel, G., Tian, F., Tong, R., Tussupova, K., 450 — Tyralis, H., Uijlenhoet, R., van Beek, R., van der Ent, R. J., van der Ploeg, M., Van Loon, A. F., van Meerveld, I., van Nooijen, R., van Oel, P. R., Vidal, J.-P., von Freyberg, J., Vorogushyn, S., Wachniew, P., Wade, A. J., Ward, P., Westerberg, I. K., White, C., Wood, E. F., Woods, R., Xu, Z., Yilmaz, K. K., and Zhang, Y.: Twenty-three unsolved problems in hydrology (UPH) – a community perspective, *Hydrological Sciences Journal*, 64, 1141–1158, <https://doi.org/10.1080/02626667.2019.1620507>, 2019.
- Bérard, P.: Alimentation en eau de la ville de Montpellier: captage de la source du Lez—étude des relations entre la source et son réservoir aquifère [Water supply of Montpellier: Lez Spring catchment—study of the relationship between the spring and its aquifer], Tech. rep., BRGM, Montpellier, France, <http://infoterre.brgm.fr/rapports/84-AGI-171-LRO-EAU.pdf>, 1983.
- 460 Chang, Y., Hartmann, A., Liu, L., Jiang, G., and Wu, J.: Identifying More Realistic Model Structures by Electrical Conductivity *Observations* of the Karst Spring, *Water Resources Research*, 57, e2020WR028587, <https://doi.org/10.1029/2020WR028587>, <https://onlinelibrary.wiley.com/doi/pdf/10.1029/2020WR028587>, 2021.
- 460 Chen, Z. and Goldscheider, N.: Modeling spatially and temporally varied hydraulic behavior of a folded karst system with dominant conduit drainage at catchment scale, Hochifen—Gottesacker, Alps, *Journal of Hydrology*, 514, 41–52, <https://doi.org/10.1016/j.jhydrol.2014.04.005>, 2014.
- 465 Chen, Z., Hartmann, A., Wagener, T., and Goldscheider, N.: Dynamics of water fluxes and storages in an Alpine karst catchment under current and potential future climate conditions, *Hydrology and Earth System Sciences*, 22, 3807–3823, <https://doi.org/10.5194/hess-22-3807-2018>, publisher: Copernicus GmbH, 2018.
- Cinkus, G., Mazzilli, N., Jourde, H., Wunsch, A., Liesch, T., Ravbar, N., Chen, Z., and Goldscheider, N.: When best is the enemy of good – critical evaluation of performance criteria in hydrological models, *Hydrology and Earth System Sciences*, 27, 2397–2411, <https://doi.org/10.5194/hess-27-2397-2023>, publisher: Copernicus GmbH, 2023a.
- Cinkus, G., Wunsch, A., Mazzilli, N., Liesch, T., Chen, Z., Ravbar, N., Doummar, J., Fernández-Ortega, J., Barberá, J. A., Andreo, B., ~~Gold-~~ 470 ~~scheider~~ **Goldscheider**, N., and Jourde, H.: Comparison of artificial neural networks and reservoir models for simulating karst spring discharge on five

a mis en forme : Retrait : Gauche : 1,22 cm, Espace Après : 0 pt, Interligne : Multiple 1,41 li, Taquets de tabulation : Pas à 18,55 cm

a mis en forme : Espace Après : 4,25 pt

a mis en forme : Retrait : Gauche : 0 cm, Suspendu : 1,2 cm, Interligne : Multiple 1,41 li

a mis en forme : Espace Après : 3,4 pt

a mis en forme : Retrait : Gauche : 1,22 cm, Espace Après : 3,4 pt, Taquets de tabulation : Pas à 18,55 cm

a mis en forme : Espace Après : 0 pt

a mis en forme : Retrait : Gauche : 0 cm, Espace Après : 3,5 pt, Taquets de tabulation : 18,55 cm, Droite

a mis en forme : Retrait : Gauche : 1,22 cm, Espace Après : 0 pt, Interligne : Multiple 1,4 li, Taquets de tabulation : Pas à 18,55 cm

a mis en forme : Espace Après : 4,25 pt

a mis en forme : Retrait : Gauche : 0 cm, Suspendu : 1,2 cm, Interligne : Multiple 1,53 li

a mis en forme : Police : 9 pt

a mis en forme : Retrait : Gauche : 0,83 cm, Suspendu : 0,35 cm, Interligne : Multiple 1,46 li

a mis en forme : Retrait : Gauche : 1,22 cm, Première ligne : 0 cm, Interligne : simple

a mis en forme : Retrait : Gauche : 0 cm, Première ligne : 0,85 cm, Espace Après : 0 pt, Interligne : Multiple

a mis en forme : Retrait : Gauche : 0,83 cm, Suspendu : 0,35 cm

a mis en forme : Retrait : Gauche : 1,22 cm, Première ligne : 0 cm, Espace Après : 3,6 pt, Interligne : Multiple 1,1 li

test sites in the Alpine and Mediterranean regions, *Hydrology and Earth System Sciences*, 27, 1961–1985, <https://doi.org/10.5194/hess475> 27-1961-2023, publisher: Copernicus GmbH, 2023b.

Clauzon, V., Mayolle, S., Leonardi, V., Brunet, P., Soliva, R., Marchand, P., Massonnat, G., Rolando, J.-P., and Pistre, S.: Fault zones in limestones: impact on karstogenesis and groundwater flow (Lez aquifer, southern France), *Hydrogeology Journal*, 475 <https://doi.org/10.1007/s10040-020-02189-9>, 2020.

Cos, J., Doblas-Reyes, F., Jury, M., Marcos, R., Bretonnière, P.-A., and Samsó, M.: The Mediterranean climate change hotspot in the CMIP5 480 and CMIP6 projections, *Earth System Dynamics*, 13, 321–340, <https://doi.org/10.5194/esd-13-321-2022>, publisher: Copernicus GmbH, 2022.

Cousquer, Y. and Jourde, H.: Reducing Uncertainty of Karst Aquifer Modeling with Complementary Hydrological Observations for the 480 Sustainable Management of Groundwater Resources, *Journal of Hydrology*, p. 128130, <https://doi.org/10.1016/j.jhydrol.2022.128130>, 2022.

485 Cousquer, Y., Sivelles, V., and Jourde, H.: Estimating the Structural Uncertainty of Lumped Parameter Models in Karst *HydrologyHydrology-ogy*: a Bayesian Model Averaging (BMA), Tech. Rep. IAHS2022-522, Copernicus Meetings, <https://meetingorganizer.copernicus.org/IAHS2022/IAHS2022-522.html>, conference Name: IAHS2022, 2022.

485 Criss, R. E. and Winston, W. E.: Do Nash values have value? Discussion and alternate proposals, *Hydrological Processes*, 22, 2723–2725, <https://doi.org/10.1002/hyp.7072>, eprint: <https://onlinelibrary.wiley.com/doi/pdf/10.1002/hyp.7072>, 2008.

490 Dakhloui, H. and Djebbi, K.: Evaluating the impact of rainfall–runoff model structural uncertainty on the hydrological rating of regional climate model simulations, *Journal of Water and Climate Change*, 12, 3820–3838, <https://doi.org/10.2166/wcc.2021.004>, 2021.

Darbandsari, P. and Coulibaly, P.: Inter-comparison of lumped hydrological models in data-scarce watersheds using different ~~pre-~~ 490 ~~cipitation~~precipitation forcing data sets: Case study of Northern Ontario, Canada, *Journal of Hydrology: Regional Studies*, 31, 100730, <https://doi.org/10.1016/j.ejrh.2020.100730>, 2020.

495 Diffenbaugh, N. S. and Giorgi, F.: Climate change hotspots in the CMIP5 global climate model ensemble, *Climatic Change*, 114, 813–822, <https://doi.org/10.1007/s10584-012-0570-x>, 2012.

Doummar, J., Sauter, M., and Geyer, T.: Simulation of flow processes in a large scale karst system with an integrated catchment 495 ~~_____~~ model (Mike She) – Identification of relevant parameters influencing spring discharge, *Journal of Hydrology*, 426-427, 112–123, <https://doi.org/10.1016/j.jhydrol.2012.01.021>, 2012.

500 Doummar, J., Hassan Kassem, A., and Gurdak, J. J.: Impact of historic and future climate on spring recharge and discharge based on an integrated numerical modelling approach: Application on a snow-governed semi-arid karst catchment area, *Journal of Hydrology*, 565, 636–649, <https://doi.org/10.1016/j.jhydrol.2018.08.062>, 2018a.

500 Doummar, J., Margane, A., Geyer, T., and Sauter, M.: Assessment of key transport parameters in a karst system under ~~differ-~~ ~~eat~~different dynamic conditions based on tracer experiments: the Jeita karst system, Lebanon, *Hydrogeology Journal*, 26, 2283–2295, 505 <https://doi.org/10.1007/s10040-018-1754-x>, 2018b.

Doummar, J., Fahs, M., Aoun, M., Elghawi, R., Othman, J., Alali, M., and Kassem, A. H.: Assessment of Water Quality and Quantity of Springs at a Pilot Scale, in: *Threats to Springs in a Changing World*, pp. 111–129, American Geophysical Union (AGU),

a mis en forme : Retrait : Gauche : 0 cm, Première ligne : 0,85 cm, Interligne : Multiple 1,44 li

a mis en forme : Retrait : Gauche : 1,22 cm, Première ligne : 0 cm, Espace Après : 3,6 pt, Interligne : Multiple 1,1 li

a mis en forme : Police :8,5 pt

a mis en forme : Retrait : Gauche : 0 cm, Suspendu : 1,2 cm, Interligne : simple

a mis en forme : Police :9 pt

a mis en forme : Retrait : Gauche : 0,85 cm, Suspendu : 0,35 cm, Espace Après : 0,85 pt, Interligne : Multiple 1,4 li

a mis en forme : Retrait : Gauche : 1,22 cm, Première ligne : 0 cm, Interligne : Multiple 1,54 li

a mis en forme : Retrait : Gauche : 0,83 cm, Suspendu : 0,35 cm, Espace Après : 0 pt, Interligne : Multiple 1,52 li

a mis en forme : Retrait : Gauche : 1,22 cm, Première ligne : 0 cm, Espace Après : 3,6 pt, Interligne : Multiple 1,1 li

a mis en forme : Retrait : Gauche : 0,83 cm, Suspendu : 0,35 cm, Espace Après : 0 pt, Interligne : Multiple 1,4 li, Taquets de tabulation : Pas à 18,55 cm

a mis en forme : Espace Après : 4,5 pt

a mis en forme : Retrait : Gauche : 1,22 cm, Première ligne : 0 cm, Espace Après : 3,6 pt, Interligne : Multiple 1,1 li

a mis en forme : Retrait : Gauche : 0,83 cm, Suspendu : 0,35 cm, Espace Après : 0 pt, Interligne : Multiple 1,4 li, Taquets de tabulation : Pas à 18,55 cm

a mis en forme : Espace Après : 4,5 pt

a mis en forme : Retrait : Gauche : 1,22 cm, Première ligne : 0 cm, Interligne : Multiple 1,52 li

a mis en forme : Retrait : Gauche : 0 cm, Première ligne : 0,85 cm, Espace Après : 0 pt, Interligne : Multiple

~~505~~ https://doi.org/10.1002/9781119818625.ch8_section: 8_eprint: https://onlinelibrary.wiley.com/doi/pdf/10.1002/9781119818625.ch8_2022

Dubois, E., Doummar, J., Pistre, S., and Larocque, M.: Calibration of a lumped karst system model and application to the Qach qouch karst spring (Lebanon) under climate change conditions, *Hydrology and Earth System Sciences*, 24, 4275–4290, <https://doi.org/https://doi.org/10.5194/hess-24-4275-2020>, publisher: Copernicus GmbH, 2020.

~~510~~ Duran, L., Massei, N., Lecoq, N., Fournier, M., and Labat, D.: Analyzing multi-scale hydrodynamic processes in karst with a coupled conceptual modeling and signal decomposition approach, *Journal of Hydrology*, 583, 124625, <https://doi.org/10.1016/j.jhydrol.2020.124625>, 2020.

Ebel, B. A. and Loague, K.: Physics-based hydrologic-response simulation: Seeing through the fog of equifinality, *Hydrological Processes*, 20, 2887–2900, <https://doi.org/10.1002/hyp.6388>, eprint: <https://onlinelibrary.wiley.com/doi/pdf/10.1002/hyp.6388>, 2006.

~~515~~ Eberhart, R. and Kennedy, J.: Particle swarm optimization, in: *Proceedings of the IEEE international conference on neural networks*, vol. 4, 515 pp. 1942–1948, Citeseer, 1995.

Elshall, A. S., Arik, A. D., El-Kadi, A. I., Pierce, S., Ye, M., Burnett, K. M., Wada, C. A., Bremer, L. L., and Chun, G.: Groundwater sustainability: a review of the interactions between science and policy, *Environmental Research Letters*, 15, 093004, <https://doi.org/10.1088/1748-9326/ab8e8c>, publisher: IOP Publishing, 2020.

~~520~~ Ferreira, P. M. d. L., Paz, A. R. d., and Bravo, J. M.: Objective functions used as performance metrics for hydrological models: state-of-the-art and critical analysis, *RBRH*, 25, e42, <https://doi.org/10.1590/2318-0331.252020190155>, 2020.

Ficchi, A., Perrin, C., and Andréassian, V.: Impact of temporal resolution of inputs on hydrological model performance: An analysis based on 2400 flood events, *Journal of Hydrology*, 538, 454–470, <https://doi.org/10.1016/j.jhydrol.2016.04.016>, 2016.

Fiorillo, F., Revellino, P., and Ventafridda, G.: Karst aquifer draining during dry periods, *Journal of Cave and Karst Studies*, 74, 148–156, ~~525~~ <https://doi.org/10.4311/2011JCKS0207>, 2012.

~~525~~ Fleury, P., Plagnes, V., and Bakalowicz, M.: Modelling of the functioning of karst aquifers with a reservoir model: Application to Fontaine de Vaucluse (South of France), *Journal of Hydrology*, 345, 38–49, <https://doi.org/10.1016/j.jhydrol.2007.07.014>, 2007.

Fleury, P., Ladouche, B., Conroux, Y., Jourde, H., and Dörfliger, N.: Modelling the hydrologic functions of a karst aquifer under active water management – The Lez spring, *Journal of Hydrology*, 365, 235–243, <https://doi.org/10.1016/j.jhydrol.2008.11.037>, 2009.

~~530~~ Ford, D. and Williams, P.: *Karst hydrogeology and geomorphology*, John Wiley & Sons, Hoboken, NJ, USA, 2013.

~~530~~ Frank, S., Goeppert, N., and Goldscheider, N.: Improved understanding of dynamic water and mass budgets of high-alpine karst systems obtained from studying a well-defined catchment area, *Hydrological Processes*, 35, e14033, <https://doi.org/10.1002/hyp.14033>, eprint: <https://onlinelibrary.wiley.com/doi/pdf/10.1002/hyp.14033>, 2021.

Freedman, D., Pisani, R., Purves, R., and Adhikari, A.: *Statistics*, WW Norton & Company New York, 2007.

~~535~~ Guinot, V., Savéan, M., Jourde, H., and Neppel, L.: Conceptual rainfall–runoff model with a two-parameter, infinite characteristic time transfer function, *Hydrological Processes*, 29, 4756–4778, <https://doi.org/10.1002/hyp.10523>, 2015.

Gupta, A. and Govindaraju, R. S.: Propagation of structural uncertainty in watershed hydrologic models, *Journal of Hydrology*, 575, 66–81, <https://doi.org/10.1016/j.jhydrol.2019.05.026>, 2019.

a mis en forme : Espace Après : 3,6 pt

a mis en forme : Retrait : Gauche : 0,84 cm, Espace Après : 4,25 pt

a mis en forme : Retrait : Gauche : 0 cm, Suspendu : 1,2 cm, Interligne : Multiple 1,41 li

a mis en forme : Retrait : Gauche : 0 cm, Première ligne : 0,85 cm, Espace Après : 0 pt, Interligne : Multiple

a mis en forme : Retrait : Gauche : 0 cm, Première ligne : 0,85 cm, Interligne : Multiple 1,52 li

a mis en forme : Retrait : Gauche : 0,83 cm, Suspendu : 0,35 cm

a mis en forme : Retrait : Gauche : 1,22 cm, Première ligne : 0 cm, Espace Après : 3,6 pt, Interligne : Multiple 1,1 li

a mis en forme : Retrait : Gauche : 0,84 cm, Espace Après : 4,25 pt

a mis en forme : Retrait : Gauche : 1,22 cm, Première ligne : 0 cm, Espace Après : 3,6 pt, Interligne : Multiple 1,1 li

a mis en forme : Espace Après : 3,4 pt

a mis en forme : Retrait : Gauche : 0 cm, Première ligne : 0,85 cm, Espace Après : 0 pt, Interligne : Multiple

570 tainty Using 36 Models and 559 Catchments, *Water Resources Research*, 56, e2019WR025975, <https://doi.org/10.1029/2019WR025975>,
_eprint: <https://onlinelibrary.wiley.com/doi/pdf/10.1029/2019WR025975>, 2020.

Labat, D., Argouze, R., Mazzilli, N., Ollivier, C., and Sivel, V.: Impact of Withdrawals on Karst Watershed Water Supply, *Water*, 14, 1339,
<https://doi.org/10.3390/w14091339>, number: 9 Publisher: Multidisciplinary Digital Publishing Institute, 2022.

575 Lee, A.: pyswarm: Particle swarm optimization (PSO) with constraint support, <https://github.com/tisimst/pyswarm>, 2014.

575 Liu, Y., Wagener, T., and Hartmann, A.: Assessing Streamflow Sensitivity to Precipitation Variability in Karst-Influenced Catchments With
Unclosed Water Balances, *Water Resources Research*, 57, e2020WR028598, <https://doi.org/10.1029/2020WR028598>, _eprint:
<https://onlinelibrary.wiley.com/doi/pdf/10.1029/2020WR028598>, 2021.

580 Lorette, G., Sebilo, M., Buquet, D., Lastennet, R., Denis, A., Peyraube, N., Charriere, V., and Studer, J.-C.: Tracing sources and fate of nitrate
in multilayered karstic hydrogeological catchments using natural stable isotopic composition ($\delta^{15}N\text{-NO}_3^-$ and $\delta^{18}O\text{-NO}_3^-$). Application
to the Toulon karst system (Dordogne, France), *Journal of Hydrology*, p. 127972, <https://doi.org/10.1016/j.jhydrol.2022.127972>, 2022.

Lukac Reberski, J., Terzić, J., Maurice, L. D., and Lapworth, D. J.: Emerging organic contaminants in karst groundwater: A global level-
assessment, *Journal of Hydrology*, 604, 127242, <https://doi.org/10.1016/j.jhydrol.2021.127242>, 2022.

Mazzilli, N., Jourde, H., Guinot, V., Bailly-Comte, V., and Fleury, P.: Hydrological modelling of a karst aquifer under active groundwater
management using a parsimonious conceptual model, H2Karst - 9th Conference on Limestone Hydrogeology, p. 4, 2011.

580 Mazzilli, N., Guinot, V., and Jourde, H.: Sensitivity analysis of conceptual model calibration to initialisation bias. Application to karst spring
discharge models, *Advances in Water Resources*, 42, 1–16, <https://doi.org/10.1016/j.advwatres.2012.03.020>, 2012.

Mazzilli, N., Jourde, H., Jacob, T., Guinot, V., Le Moigne, N., Boucher, M., Chalikhakis, K., Guyard, H., and Legtchenko, A.: On the inclusion of
ground-based gravity measurements to the calibration process of a global rainfall-discharge reservoir model: case of the Durzon karst
590-system (Larzac, southern France), *Environmental Earth Sciences*, 68, 1631–1646, <https://doi.org/10.1007/s12665-012-1856-z>, 2013.

585 Mazzilli, N., Guinot, V., Jourde, H., Lecoq, N., Labat, D., Arfib, B., Baudement, C., Danquigny, C., Dal Soglio, L., and Bertin, D.: KarstMod: A
modelling platform for rainfall - discharge analysis and modelling dedicated to karst systems, *Environmental Modelling & Software*, 122,
103927, <https://doi.org/10.1016/j.envsoft.2017.03.015>, 2019.

Mazzilli, N., Sivel, V., Cinkus, G., Jourde, H., and Bertin, D.: KarstMod User Guide - version 3.0, 2022.

595 McMillan, H., Jackson, B., Clark, M., Kavetski, D., and Woods, R.: Rainfall uncertainty in hydrological modelling: An evaluation of multi-
multi590 plicative error models, *Journal of Hydrology*, 400, 83–94, <https://doi.org/10.1016/j.jhydrol.2011.01.026>, 2011.

Moges, E., Demissie, Y., Larsen, L., and Yassin, F.: Review: Sources of Hydrological Model Uncertainties and Advances in Their Analysis,
Water, 13, 28, <https://doi.org/10.3390/w13010028>, number: 1 Publisher: Multidisciplinary Digital Publishing Institute, 2021.

Moriasi, D. N., Arnold, J. G., Liew, M. W. V., Bingner, R. L., Harmel, R. D., and Veith, T. L.: Model Evaluation Guidelines for Systematic
600-Quantification of Accuracy in Watershed Simulations, *Transactions of the ASABE*, 50, 885–900, <https://doi.org/10.13031/2013.23153>,
595 2007.

Nash, J. E. and Sutcliffe, J. V.: River flow forecasting through conceptual models part I — A discussion of principles, *Journal of Hydrology*, 10,
282–290, [https://doi.org/10.1016/0022-1694\(70\)90255-6](https://doi.org/10.1016/0022-1694(70)90255-6), 1970.

Nerantzaki, S. D. and Nikolaidis, N. P.: The response of three Mediterranean karst springs to drought and the impact of climate change, 605
Journal of Hydrology, 591, 125296, <https://doi.org/10.1016/j.jhydrol.2020.125296>, 2020.

a mis en forme : Retrait : Gauche : 0 cm, Suspendu :
1,2 cm, Interligne : Multiple 1,41 li

a mis en forme : Retrait : Gauche : 0,84 cm, Espace
Après : 4,5 pt

a mis en forme : Retrait : Gauche : 0 cm, Suspendu :
1,2 cm, Interligne : Multiple 1,48 li

a mis en forme : Retrait : Gauche : 0,83 cm, Suspendu :
0,35 cm, Interligne : Multiple 1,4 li

a mis en forme : Retrait : Gauche : 1,22 cm, Première
ligne : 0 cm, Espace Après : 3,6 pt, Interligne : Multiple
1,1 li

a mis en forme : Retrait : Gauche : 0,83 cm, Suspendu :
0,35 cm

a mis en forme : Retrait : Gauche : 0 cm, Suspendu :
1,2 cm, Interligne : Multiple 1,46 li

a mis en forme : Espace Après : 3,4 pt

a mis en forme : Retrait : Gauche : 0 cm, Première
ligne : 0,85 cm, Interligne : Multiple 1,52 li

a mis en forme : Espace Après : 3,4 pt

a mis en forme : Retrait : Gauche : 0 cm, Première
ligne : 0 cm, Espace Après : 3,55 pt, Interligne : Multiple
1,1 li, Taquets de tabulation : 1,56 cm, Centré

a mis en forme : Retrait : Gauche : 0,83 cm, Suspendu :
0,35 cm

600 Ollivier, C., Mazzilli, N., Olioso, A., Chalikakis, K., Carrière, S. D., Danquigny, C., and Emblanch, C.: Karst rechargedischarge semi distributed model to assess spatial variability of flows, Science of The Total Environment, 703, 134368, <https://doi.org/10.1016/j.scitotenv.2019.134368>, 2020.

a mis en forme : Retrait : Gauche : 0 cm, Suspendu : 1,2 cm, Interligne : Multiple 1,41 li

Oudin, L., Hervieu, F., Michel, C., Perrin, C., Andréassian, V., Anctil, F., and Loumagne, C.: Which potential evapotranspiration input for a lumped rainfall–runoff model? Part 2—Towards a simple and efficient potential evapotranspiration model for rainfall–runoff modelling,

a mis en forme : Police :9 pt

605 Journal of Hydrology, 303, 290–306, <https://doi.org/10.1016/j.jhydrol.2004.08.026>, 2005.

a mis en forme : Retrait : Gauche : 0 cm, Première ligne : 0,85 cm, Interligne : Multiple 1,46 li

Oudin, L., Perrin, C., Mathevet, T., Andréassian, V., and Michel, C.: Impact of biased and randomly corrupted inputs on the efficiency and the parameters of watershed models, Journal of Hydrology, 320, 62–83, <https://doi.org/10.1016/j.jhydrol.2005.07.016>, 2006.

~~Palmer, A. N.: Origin and morphology of limestone caves, Geological Society of America Bulletin, 103, 1–21, 1991.~~

615 Pandi, D., Kothandaraman, S., and Kuppasamy, M.: Hydrological models: a review, International Journal of Hydrology Science and Technology, 12, 223–242, <https://doi.org/10.1504/IJHST.2021.117540>, publisher: Inderscience Publishers, 2021.

a mis en forme : Retrait : Gauche : 0,83 cm, Suspendu : 0,35 cm, Espace Après : 0 pt, Interligne : Multiple 1,52 li

610 Pechlivanidis, I., Jackson, B., McMillan, H., and Gupta, H. V.: Using an informational entropy-based metric as a diagnostic of flow duration to drive model parameter identification, Global NEST Journal, 14, 325–334, <https://doi.org/10.30955/gnj.000879>, 2013.

a mis en forme : Retrait : Gauche : 1,22 cm, Première ligne : 0 cm, Espace Après : 3,6 pt, Interligne : Multiple 1,1 li

Perrin, C., Michel, C., and Andréassian, V.: Does a large number of parameters enhance model performance? Comparative assessment of common catchment model structures on 429 catchments, Journal of Hydrology, 242, 275–301, [https://doi.org/10.1016/S00221694\(00\)00393-0](https://doi.org/10.1016/S00221694(00)00393-0), 2001.

a mis en forme : Retrait : Gauche : 0,83 cm, Suspendu : 0,35 cm, Interligne : Multiple 1,46 li

615 Pianosi, F., Sarrazin, F., and Wagener, T.: A Matlab toolbox for Global Sensitivity Analysis, Environmental Modelling & Software, 70, 80–85, <https://doi.org/10.1016/j.envsoft.2015.04.009>, 2015.

~~Pianosi, F., Sarrazin, F., and Wagener, T.: How successfully is open-source research software adopted? Results and implications~~
625 ~~implications~~ of surveying the users of a sensitivity analysis toolbox, Environmental Modelling & Software, 124, 104579, <https://doi.org/10.1016/j.envsoft.2019.104579>, 2020.

a mis en forme : Retrait : Gauche : 0,83 cm, Suspendu : 0,35 cm, Espace Après : 0 pt, Interligne : simple, Taquets de tabulation : Pas à 18,55 cm

a mis en forme : Espace Après : 4,5 pt

620 Pool, S., Vis, M., and Seibert, J.: Evaluating model performance: towards a non-parametric variant of the Kling-Gupta efficiency, Hydrological Sciences Journal, 63, 1941–1953, <https://doi.org/10.1080/02626667.2018.1552002>, 2018.

a mis en forme : Retrait : Gauche : 1,22 cm, Première ligne : 0 cm, Espace Après : 3,6 pt, Interligne : Multiple 1,1 li

Poulain, A., Watlet, A., Kaufmann, O., Van Camp, M., Jourde, H., Mazzilli, N., Rochez, G., Deleu, R., Quinif, Y., and Hallet, V.: Assessment of groundwater recharge processes through karst vadose zone by cave percolation monitoring, Hydrological Processes, 32, 2069–2083, <https://doi.org/10.1002/hyp.13138>, 2018. <https://doi.org/10.1002/hyp.13138>, 2018.

a mis en forme : Retrait : Gauche : 0,83 cm, Suspendu : 0,35 cm, Espace Après : 0 pt, Interligne : Multiple 1,46 li, Taquets de tabulation : Pas à 18,55 cm

625 Sarrazin, F., Hartmann, A., Pianosi, F., Rosolem, R., and Wagener, T.: V2Karst V1.1: a parsimonious large-scale integrated vegetation-recharge model to simulate the impact of climate and land cover change in karst regions, Geoscientific Model Development, 11, 4933–4964, <https://doi.org/10.5194/gmd-11-4933-2018>, 2018.

a mis en forme : Retrait : Gauche : 1,22 cm, Première ligne : 0 cm, Interligne : Multiple 1,52 li

625 Schilling, O. S., Cook, P. G., and Brunner, P.: Beyond Classical Observations in Hydrogeology: The Advantages of Including Exchange Flux, Temperature, Tracer Concentration, Residence Time, and Soil Moisture Observations in Groundwater Model Calibration, Reviews of Geophysics, <https://doi.org/10.1029/2018rg000625>, 2018.

[630 physics](https://doi.org/10.1029/2018RG000619), 57, 146–182, <https://doi.org/10.1029/2018RG000619>, _eprint: <https://onlinelibrary.wiley.com/doi/pdf/10.1029/2018RG000619>, 2019.

Schwemmler, R., Demand, D., and Weiler, M.: Technical note: Diagnostic efficiency – specific evaluation of model performance, *Hydrology and Earth System Sciences*, 25, 2187–2198, <https://doi.org/10.5194/hess-25-2187-2021>, publisher: Copernicus GmbH, 2021.

Shmueli, G.: To Explain or to Predict?, *Statistical Science*, 25, 289–310, <https://doi.org/10.1214/10-STS330>, publisher: Institute of Mathematical Statistics, 2010.

Sivelle, V. and Jourde, H.: A methodology for the assessment of groundwater resource variability in karst catchments with sparse temporal measurements, *Hydrogeology Journal*, 29, 137–157, <https://doi.org/10.1007/s10040-020-02239-2>, 2020.

[645](https://doi.org/10.1016/j.jhydrol.2021.126396) Sivelle, V., Labat, D., Mazzilli, N., Massei, N., and Jourde, H.: Dynamics of the Flow Exchanges between Matrix and Conduits in Karstified Watersheds at Multiple Temporal Scales, *Water*, 11, 569, <https://doi.org/10.3390/w11030569>, 2019.

[640](https://doi.org/10.1016/j.jhydrol.2021.126396) Sivelle, V., Jourde, H., Bittner, D., Mazzilli, N., and Trambly, Y.: Assessment of the relative impacts of climate changes and anthropogenic forcing on spring discharge of a Mediterranean karst system, *Journal of Hydrology*, 598, 126396, <https://doi.org/10.1016/j.jhydrol.2021.126396>, 2021.

[650](https://doi.org/10.1016/j.jhydrol.2022.128264) Sivelle, V., Jourde, H., Bittner, D., Richieri, B., Labat, D., Hartmann, A., and Chiogna, G.: Considering land cover and land use (LCLU) in lumped parameter modeling in forest dominated karst catchments, *Journal of Hydrology*, 612, 128264, <https://doi.org/10.1016/j.jhydrol.2022.128264>, 2022a.

Sivelle, V., Pérotin, L., Ladouche, B., de Montety, V., Bailly-Comte, V., Champollion, C., and Jourde, H.: A lumped parameter model to evaluate the relevance of excess air as a tracer of exchanged flows between transmissive and capacitive compartments of karst systems, *Frontiers in Water*, 4, <https://www.frontiersin.org/articles/10.3389/frwa.2022.930115>, 2022b.

Smiatek, G., Kaspar, S., and Kunstmann, H.: Hydrological Climate Change Impact Analysis for the Figeih Spring near Damascus, Syria, *Journal of Hydrometeorology*, 14, 577–593, <https://doi.org/10.1175/JHM-D-12-065.1>, publisher: American Meteorological Society Section: Journal of Hydrometeorology, 2013.

Sobol, I. M.: Uniformly distributed sequences with an additional uniform property, *USSR Computational Mathematics and Mathematical Physics*, 16, 236–242, [https://doi.org/10.1016/0041-5553\(76\)90154-3](https://doi.org/10.1016/0041-5553(76)90154-3), 1976.

[Sophocleous, M.: Interactions between groundwater and surface water: the state of the science, *Hydrogeology Journal*, 10, 52–67, 655 https://doi.org/10.1007/s10040-001-0170-8, 2002.](https://doi.org/10.1007/s10040-001-0170-8)

Stevanovic, Z.: Karst waters in potable water supply: a global scale overview, *Environmental Earth Sciences*, 78, 662, <https://doi.org/10.1007/s12665-019-8670-9>, 2019.

[Wada, Y., Florke, M., Hanasaki, N., Eisner, S., Fischer, G., Tramberend, S., Satoh, Y., van Vliet, M. T. H., Villia, P., Ringler, C., Burek, P., and Wiberg, D.: Modeling global water use for the 21st century: the Water Futures and Solutions \(WFaS\) initiative and its approaches, *Geoscientific Model Development*, 9, 175–222, <https://doi.org/10.5194/gmd-9-175-2016>, 2016.](https://doi.org/10.5194/gmd-9-175-2016)

Westerberg, I. K., Sikorska-Senoner, A. E., Viviroli, D., Vis, M., and Seibert, J.: Hydrological model calibration with uncertain discharge data, *Hydrological Sciences Journal*, 0, null, <https://doi.org/10.1080/02626667.2020.1735638>, publisher: Taylor & Francis _eprint: <https://doi.org/10.1080/02626667.2020.1735638>, 2020.

a mis en forme : Interligne : simple

a mis en forme : Retrait : Gauche : 0,83 cm, Suspensio : 0,35 cm

a mis en forme : Retrait : Gauche : 0 cm, Première ligne : 0,85 cm, Interligne : Multiple 1,5 li

a mis en forme : Retrait : Gauche : 0,83 cm, Suspensio : 0,35 cm, Interligne : Multiple 1,52 li

a mis en forme : Espace Après : 3,6 pt

a mis en forme : Retrait : Gauche : 0 cm, Première ligne : 0,85 cm, Espace Après : 0 pt, Interligne : Multiple

a mis en forme : Retrait : Gauche : 0,83 cm, Suspensio : 0,35 cm

a mis en forme : Retrait : Gauche : 0 cm, Première ligne : 0,85 cm

a mis en forme : Retrait : Gauche : 0,83 cm, Suspensio : 0,35 cm

a mis en forme : Retrait : Gauche : 0 cm, Première ligne : 0,85 cm, Interligne : Multiple 1,51 li

~~White, W. B.: Conceptual models for karstic aquifers, Karst modeling, 5, 11–16, publisher: Karst Waters Institute Special Publication Charles
670 Town, West Virginia, 1999.~~

Zhou, S., Wang, Y., Li, Z., Chang, J., and Guo, A.: Quantifying the Uncertainty Interaction Between the Model Input and Structure on Hydrological Processes, *Water Resources Management*, 35, 3915–3935, <https://doi.org/10.1007/s11269-021-02883-7>, 2021.

Çallı, S. S., Çallı, K., Tugrul Yılmaz, M., and Çelik, M.: Contribution of the satellite-data driven snow routine to a karst hydrological model, *Journal of Hydrology*, 607, 127511, <https://doi.org/10.1016/j.jhydrol.2022.127511>, 2022.